UNIVERSITY OF CALIFORNIA SAN DIEGO

Chemical Genetics Investigation of DFPM-triggered Biotic and Abiotic Stress Signaling in *A. thaliana*

A thesis submitted in partial satisfaction of the requirements for the degree Master of Science

in

Biology

By

Chia-Yu Tsai

Committee in charge:

Professor Julian I. Schroeder, Chair
Professor Alisa Huffaker
Professor Yunde Zhao

2019

The Thesis of Chia-Yu Tsai is approved, and it is acceptable in quality and form for publication on microfilm and electronically:

_____

_____

_____

Chair

University of California San Diego

2019

DEDICATION

給我親愛的爸爸[蔡台豐], 媽媽[楊智蘭], 與哥哥[蔡一平]

只有誠心一句

謝謝你

TABLE OF CONTENTS

LIST OF FIGURES

LIST OF TABLES

ACKNOWLEDGMENTS

I would like to acknowledge Professors Julian Schroeder, Yunde Zhao, and Alisa Huffaker for their support as the chairs of my committee. Their continuous guidance through my undergraduate and graduate education, research, and personal growth have been selfless, powerful, and invaluable.

I would like to acknowledge Dr. Jiyoung Park and Dr. Po-Kai Hsu for their support as my post-doctoral mentors throughout my time in the Schroeder Lab. Their repeated belief in me kept me humble and grounded each day in the laboratory, a non-successful experiment after another.

I would like to acknowledge my colleagues Eduardo Ramirez, Alex Scavo, Shannon Laub, and Alexandre Miaule for the company and guidance especially during the late nights, weekends, and experimental disasters. It is their support and entertainment that helped maintain my morale through those particularly difficult times.

I would like to acknowledge Schroeder Lab members Drs. Alyona Bobkova, Andrew Cooper, Felix Hauser, Paulo Ceciliato, Guillaume Dubeaux, Chuck Seller, and Sebastian Schulz for serving as inspirational pillars of knowledge in the laboratory. It is their fountain of knowledge and compassionate teaching that continues to push me into the field of science and education.

ABSTRACT OF THE THESIS

Chemical Genetics Investigation of DFPM-triggered Biotic and Abiotic Stress Signaling in *A. thaliana*

by

Chia-Yu Tsai

Master of Science in Biology

University of California San Diego, 2019

Professor Julian I. Schroeder, Chair

Being sessile organisms, plants have evolutionarily developed a variety of mechanisms to protect themselves from biotic and abiotic stressors such as pathogen exposure, drought conditions, and heavy metal contamination. The phytohormone, abscisic acid (ABA), is a major stress hormone in *Arabidopsis thaliana* essential for resistance to abiotic stressors, such as drought conditions. In addition to mediating drought tolerance, however, ABA has been found to interfere with pathogen resistance signaling as well by increasing susceptibility to pathogens. Recent discoveries demonstrated a novel interference in plant stress signaling-- ABA signal repression by pathogen defense activation by the small molecule [5-(3,4-dichlorophenyl)furan-2-yl]- piperidine-1-yl methanethione (DFPM). In Chapter 1, fluorescence microscopy and genetic analysis

techniques are utilized in attempts to identify a mutant found to be resistant to DFPM inhibition of ABA signal transduction. Experimental findings include a growth phenotype of this mutant and approximate candidate genes of the *rda1* causative mutation. In Chapter 2, a novel chemical genetics screen utilizing an artificial microRNA library was developed to identify genetic components necessary for a DFPM induced root-specific meristematic cell death signaling pathway. Study findings include the establishment of a robust chemical genetics screen, demonstration of mutant phenotypes, and identification of a DFPM-resistant mutant candidate which repeatedly demonstrated a root growth continuation phenotype.

Chapter 1

Investigating the Resistant to DFPM-inhibition of ABA (*rda)-1* Mutant

1.1 Introduction

In its most recent 2019 report, the Food and Agriculture Organization of the United Nations (FAO) draws attention to the plight of human health and its grim future in consequence to the current climate changes. Each year, agriculture faces a number of environmental stressors, biotic and abiotic, that can harm its quantity and quality. While plants face specific types of stressors depending on location, climate, and age, they uniformly take precautionary measures with the similar outcomes of energy preservation and damage control (Foyer *et al.*, 2 016). Further exploration of the various stress resistance and regulatory mechanisms developed in plants will allow for better future development of food sustainability and security in the ever-changing climate.

When responding to its environmental stressors, plants commonly activate specific but overlapping metabolic or immune signaling pathways depending on the type of stressor (Atkinson and Urwin, 2012). The types of stressors can be broadly organized into biotic or abiotic stressors. Biotic stressors include factors from other living organisms such as insects, fungi, bacteria, or plants. Contrasting, abiotic stressors include factors from non-living organisms such as drought conditions, heavy metal and salinity contamination, or temperature extremes (Deinlin *et al.*, 2014; Assmann *et al.*, 2013). The plant responses to these individual stressors have been extensively studied in the past to build the foundations of today's knowledge. (Need to Expand)

Realistically, however, plants often are exposed to multiple stresses, instead of individual stressors at a time. As a result, plants have developed the capacity to recognize and respond appropriately to biotic and abiotic environmental variables by fine tuning their metabolic and

immune signaling to maintain survival in a competitive environment (Foyer *et al*., 2016). In fact, studies building on fundamental research findings have demonstrated a cross-tolerance phenomena when pairing different environmental stressors. Cross-tolerance phenomena are defined as an enhanced tolerance to a range of different environmental stressors triggered by the exposure to a single stress (Foyer *et al*., 2016, Pastori and Foyer, 2002, Mittler, 2006, Choudhury *et al*., 2016). This phenomenon is achieved by synergistic co-activation of plant immune response pathways that encompass both biotic and abiotic stress boundaries (Bostock, 2005).

Of particular recent interest, is the cross-tolerance signaling that occurs between the abiotic and biotic stressors, drought tolerance and pathogen infection, respectively. Under recognition of drought conditions, signaling pathways are activated to close stomatal pores and down-regulate vegetative growth. Commonly, this is accomplished by the endogenous production of the major abiotic stress hormone, abscisic acid (ABA). Beyond drought response signaling, ABA has been widely studied and found to regulate several other important aspects of plant growth and development such as seed dormancy, initiation of senescence, and inhibition of growth-promoting hormones under salt and cold stress (Nakashima *et al*., 2013; Finkelstein *et al*., 2002, Kim *et al*., 2010).

ABA has also been extensively characterized as a major hormone essential to resistance to drought conditions by initiating stomatal pore closure in plant leaves to reduce water loss (Cutler *et al*., 2010, Finkelstein *et al*., 2013, Hauser *et al*., 2017). In addition to drought signaling, multiple literature sources have demonstrated ABA's involvement in a novel interference in plant stress signaling, which can depend on the type of pathogen (Audenaert *et al.,* 2002, Kim *et al.,* 2011, Park *et al.,* 2019). Instead of a cross-tolerance phenomenon where

the immunity to secondary stressors are enhanced by the activation of a singular stress signal, researchers repeatedly demonstrate the inhibition of ABA signaling by pathogen defense activation (Audenaert *et al*., 2002, Mohr *et al*., 2003, Asselbergh *et al*., 2008, Kim *et al*., 2011). However, because pathogen infection mechanisms vary and result in respective complex immune signaling pathways, standardizing and imitating natural pathogen infection conditions under both drought conditions has proven to be difficult.

To consistently and robustly imitate natural pathogen infection conditions, we are utilizing a chemical tool identified and validated in Julian Schroeder's lab as a chemical that activates immune signaling mechanisms, to examine the novel interference of biotic to abiotic stress. In a chemical genetics approach it was found that exposure to a novel small molecule, [5-(3,4-dichlorophenyl)furan-2-yl]- piperidine-1-yl methanethione (DFPM), down-regulates ABA-signaling while up-regulating pathogen resistance signaling pathways in plants, proving to be a possible tool to further elucidate cross-interference in plant stress signaling (Kim *et al*., 2012, Kim *et al*., 2011). Kim and colleagues demonstrated that DFPM inhibits ABA-mediated effects including gene expression, slow-type anion channel activation, and stomatal closure, all while upregulating various effector-triggered immunity responses (Kim *et al*., 2011). Thus far, research has indicated a DFPM requirement of core genetic components of effector-triggered immunity including EDS1(Effector Disease Susceptibility 1), PAD 4(Phytoalexin Deficient 4), RAR1(Required for Mla1 Resistance), and SGT1b(Suppressor of the G2 Allele of *skp1 1b)* for a DFPM mediated inhibition of ABA signaling (Kim et al. 2011) and for a DFPM mediated root specific root growth arrest response (Kim *et al*., 2012; Kunz *et al*., 2016). These recent studies establish DFPM as a tool to further investigate this pathogen resistance signaling dependent inhibition of ABA signal transduction.

To further elucidate this novel signal interference, a large-scale chemical genetic mutant screening for DFPM insensitivity was conducted utilizing Arabidopsis thaliana (Park *et al*., 2019, Kunz *et al*., 2016). Park and colleagues isolated 3 ethyl methanesulfonate (EMS) - mutagenized mutants that were resistant to DFPM inhibition of ABA signaling, named *rda1*, *rda2,* and *rda3* (Resistant to DFPM Inhibition of ABA). *rda2,* demonstrating the strongest resistant to DFPM inhibition of ABA phenotype, has been mapped to a lectin receptor kinase, demonstrated to play role in biotic stress reception (Park *et al*.,2019). In addition to the resistant to DFPM inhibition phenotype, the lectin receptor kinase has been identified to facilitate the activation of mitogen-activated protein kinase (MPK) 3 and 6 signaling activation by DFPM (Park et al., 2019). On the other hand, has not been mapped and remains uncharacterized.

Here we demonstrate efforts of mapping the *rda1* mutation via bulk segregant analysis and whole genome sequencing. Although we have not mapped the *rda1* causative mutation, we have narrowed down the list of possible mutations and identified additional phenotypes for *rda1* that will be of interest to future research exploring DFPM inhibition of ABA signaling.

1.2 Materials and Methods

Plant Material and Growth Conditions

Seeds were surface sterilized with 70% Ethanol for 15 minutes, rinsed with 100% Ethanol five times, then plated onto ½ Murashige and Skoog, 1% Sucrose, 0.8% agar media, pH 5.8 media. Plates were then placed in the dark at 4°C for 48-72 hours of cold treatment before transfer to a 16/8h light/dark growth chamber at 21°C.

Whole Genome Sequencing

Plants used for bulk segregant analysis were 11 plants from the F3 backcrossed *rda1 pRAB18::GFP* lines. DNA was isolated via DNeasy Plant kit (Qiagen) and quantified via Qubit dsDNA HS Assay kit (Thermo Fischer Scientific). Equal amounts of gDNA from the 11 lines were then pooled together for whole-genome sequencing. Approximately 110 ng of gDNA was tagmented using the Nextera DNA Sample Preparation Kit (Illumina) with 0.5 ml Tn5 (Tagment DNA Enzyme 1) in a total volume of 20 ul and 5 min incubation time at 55 °C. Reaction was purified using the ChIP DNA Clean and Concentrate kit (Zymo Research) and amplified and barcoded for 4 PCR cycles. Libraries were size selected for 200-250bp by gel isolation and sequenced SE75 on a NextSeq 2500 (Illumina). Sequence analysis was conducted via the SIMPLE Pipeline protocol (Benfey *et al.,* 2017). By comparing *rda1 pRAB18::GFP* sequence with Col-0 pRAB18::GFP parental line sequence, occurrence ratios for the genome were graphed via MATLAB with moving averages of 10.

Fluorescence Microscopy

Seeds were grown following conditions listed above in "*Plant Material and Growth Conditions*". On day 7 after transfer to 16/8h growth chamber, seedlings were transferred to potting soil and grown in a separate 12/12h light/dark growth chamber at 21°C. On day 14, the first and second true leaves were removed and placed, with the abaxial side interfacing the media, into 24-well plates containing ½ Murashige and Skoog, 1% sucrose. To each well, 10µM of DFPM or 0.06% DMSO control was added first. After 1 hour of treatment, 20µM ABA or Ethanol control was added. After 24h of both treatments, the abaxial surface of chemically treated leaves were visualized with a confocal microscope with respective fluorescence. Constant gain and exposure times were utilized for the experimental imaging and data comparison. The image analyses were conducted via ImageJ software (Elicieri *et al*., 2017).

Map Kinase Assays

Seedlings were grown following the conditions listed above in "*Plant Material and Growth Conditions*". On day 14 of growth on the ½ Murashige and Skoog, 1% sucrose, and 0.8% agar media, entire seedlings with roots were transferred to 24-well plates containing ½ Murashige and Skoog, 1% sucrose, containing 30µM DFPM or 0.06% DMSO (solvent control) for 0, 15, and 30 minutes. Total proteins were extracted via extraction buffer [25 mM Tris-HCl (pH 7.8), 75 mM NaCl, 10 mM $MgCl_2$, 15 mM EGTA, 1 mM dithiothreitol (DTT), 1 mM NaF, 0.5 mM $NaVO_3$, 15 mM β-glycerolphosphate, 15 mM p-nitrophenylphosphate, 0.1% Tween 20, 0.5 mM phenylmethylsulfonyl fluoride, 5 µg ml^{-1} leupeptin]. 20µg of total protein from each treatment and genotype were subjected to SDS-PAGE. Western blot was performed with

antibody [anti-phospho-p44/42 MAPK (Erk1/2) (Thr202/Tyr204)] and secondary anti-rabbit antibody. The blots were stained with coomassie blue dye to visualize total protein sample in each well.

1.3 Results

Building off of prior findings of the resistant to DFPM-inhibition of ABA (rda) phenotype, we repeated microscopy and map kinase phosphorylation assays for isolated *rda1* mutants to confirm and test for possible differences contrasting *rda2* (Park *et al.*, 2019). Following, we followed up on prior attempts of mutant mapping via bulk segregant analysis.

Repeating the rda1 resistant to DFPM-inhibition of ABA-mediated pRAB18::GFP Phenotype

GFP fluorescence of *rda1 pRAB18::GFP*, *rda2 pRAB18::GFP*, and WT Col-0 pRAB18::GFP were compared 24h after control, ABA, and DFPM followed by ABA chemical treatments. Both *rda1* and *rda2* demonstrated a resistant to DFPM-inhibition of ABA-mediated pRAB18::GFP fluorescence, with *rda2* demonstrating a more significant resistance (***$p<0.001$, Figure 1.1) than *rda1* (*$p<0.01$, Figure 1.1). This confirms the resistant to DFPM inhibition of ABA phenotype in the currently utilized *rda1* seeds, and repeats the published resistant to DFPM inhibition of ABA phenotype in *rda2*.

Rda1 Whole Genome Sequencing and mutant mapping

Plants were selected for *rda1* mutant mapping utilizing a similar crossing and selection method as *rda2* (Park *et al.*, 2019). The first attempt at whole genome sequencing occurred prior to my joining the Schroeder laboratory by Dr. Jiyoung Park. Dr. Park screened 120 BC1F2 out of over 760 *rda1 pRAB18::GFP* plants that demonstrated a resistant to DFPM inhibition of ABA signaling phenotype for bulk segregant analysis. The whole genome sequencing results of *rda1 pRAB18::GFP* BC1F2 were compared to sequencing results of pooled parental Col-0 pRAB18::GFP and no clear enriched interval in the *rda1 pRBA18::GFP* genome was identified

(Figure 1.3). Following, 77 BC1F3 were retested and only 11 BC1F3 demonstrated a resistant to DFPM-inhibition of ABA phenotype. The 11 lines from BC1F3 were utilized this time for a second attempt at bulk-segregant analysis. Equal amounts of DNA from the 11 BC1F3 mutants were pooled and sent for Next Generation sequencing, in comparison to DNA from the parental line of Col-0 pRAB1. Whole genome sequencing results were analyzed via isolation of EMS-type Single Nucleotide Polymorphisms (SNP), plotting of mutant occurrence ratios, and identification of effective mutations (Table 1.1). The total occurrence ratios plotted across the 5 chromosomes of *A. thaliana* indicated two peaks in chromosomes 2 and 4 (Figure 1.4). Focusing on these peak regions, EMS-type SNP's were identified by choosing for mutations in the mutant sequence where base pairs cytosine and guanine were altered to thymine and adenine, respectively (Table 1.1). Between the 2 peaks, a total of 14 mutations were identified to lead to amino acid substitutions or premature stop codons (Table 1.2).

T-DNA insertion mutant lines for each of the 14 *rda1* candidate mutations were utilized to begin mapping for *rds1*. So far, 3 mutant lines were grown and tested in order of decreasing mutant occurrence ratios: Nuclear Pore Complex Protein 58 (NUP58) At4g37130 at mutant ratio of 1.00, Nodule Inception Protein-like Protein 1 (NIN-like protein1) At2g17510 at mutant ratio of 0.944, Early-Responsive to Dehydration 7 (ERD7) At2g17840 at mutant ratio of 0.909 (Table 1.2). Homozygous lines of NUP58, NIN1, and ERD7 were isolated for crossing with *rda1 pRAB18::GFP*, to test for allelism between the T-DNA mutant lines and *rda1*. We were unsuccessful in crossing *rda1* and the homozygous mutant lines but confirmed a stunted growth phenotype and early flowering phenotype (Figure 1.4)

MAP Kinase Activation

Previously, Kim demonstrated DFPM signaling requires immune signaling components EDS1, PAD4, SGT1b, and RAR-1 (Kim *et al*., 2011; Kim *et al*., 2012; Kunz *et al*., 2016). Yet, Park demonstrated DFPM induction of MAP kinase 3 and 6 phosphorylation and gene expression in a RDA2-requiring pathway separate or downstream from the EDS1, PAD4, SGT1b, and RAR-1 signaling transduction pathways (Park *et al*., 2019).

Taking into account the *rda2* mutant findings, we analyzed whether DFPM activation of MPK3 and MPK6 were also reduced in *rda1* mutants (Figure). Contrasting the *rda2* mutant phenotype, however, *rda1* does not have a decreased MPK3/6 phosphorylation when treated with DFPM. At time 15 and 30 minutes, *rda1* mutants demonstrated a wild-type like MPK3/6 phosphorylation that is increased compared to *rda2*.

A

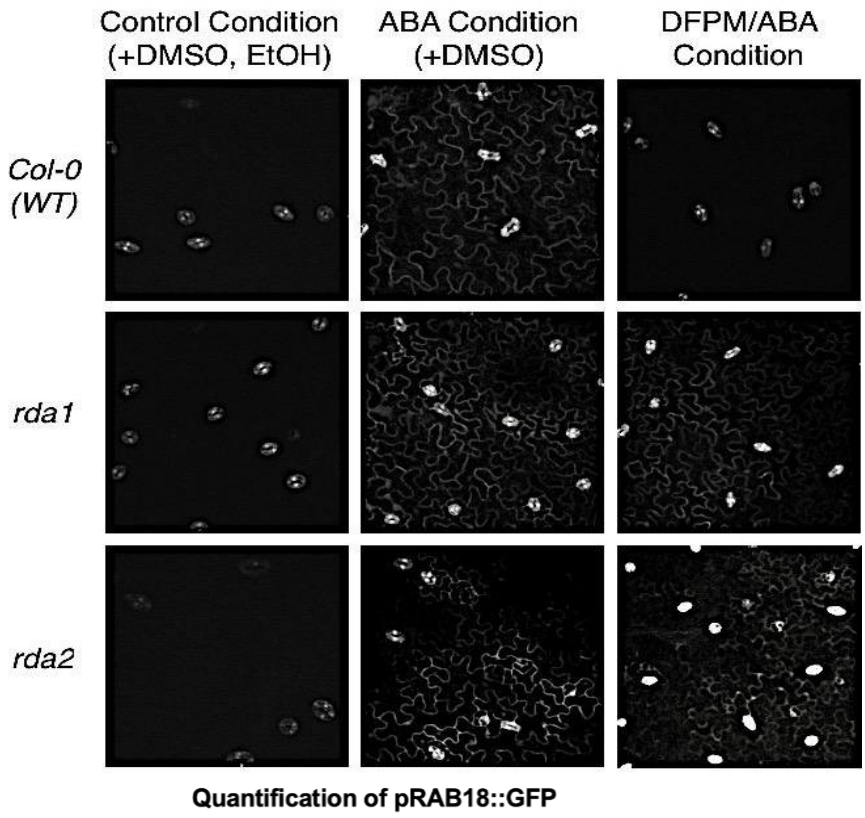

B

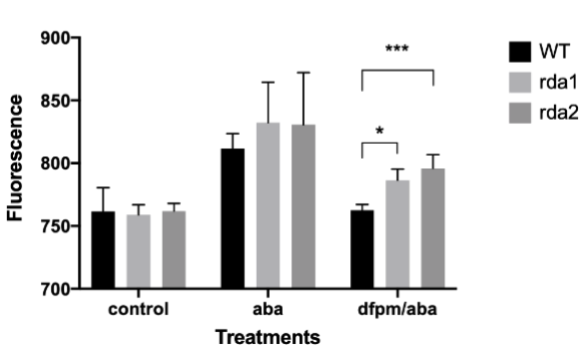

Figure 1.1: *rda1 pRAB18::GFP* Fluorescence phenotype was captured via confocal imaging, quantified via ImageJ, and statistically analyzed via Prism. Both mutants *rda1 pRAB18::GFP* and *rda2 pRAB18::GFP* demonstrates a resistance to DFPM inhibition of ABA-mediated pRAB18::GFP fluorescence. (a) Images of the epidermal pavement cells and stomata on the abaxial surface of the 1st and 2nd true leaves. Each leaf was first treated with 10 μM DFPM for 1 hour, then 20 μM ABA for 24 hours prior to microscopy. *rda1* and *rda2* both demonstrated the resistant to DFPM inhibition of ABA phenotype whereas Col-0 (WT) demonstrated DFPM inhibition of ABA-mediated pRAB18::GFP fluorescence. (b) Fluorescence quantifications in control conditions and ABA were not statistically significant across the three genotypes. Only in DFPM/ABA treatment, *rda1* and WT demonstrated a statistical difference, * $p<0.01$, and *rda2* contrasted WT, *** $p<0.001$. n = 2 experiments, with the averages of 9-22 images per genotype and condition were plotted in this figure.

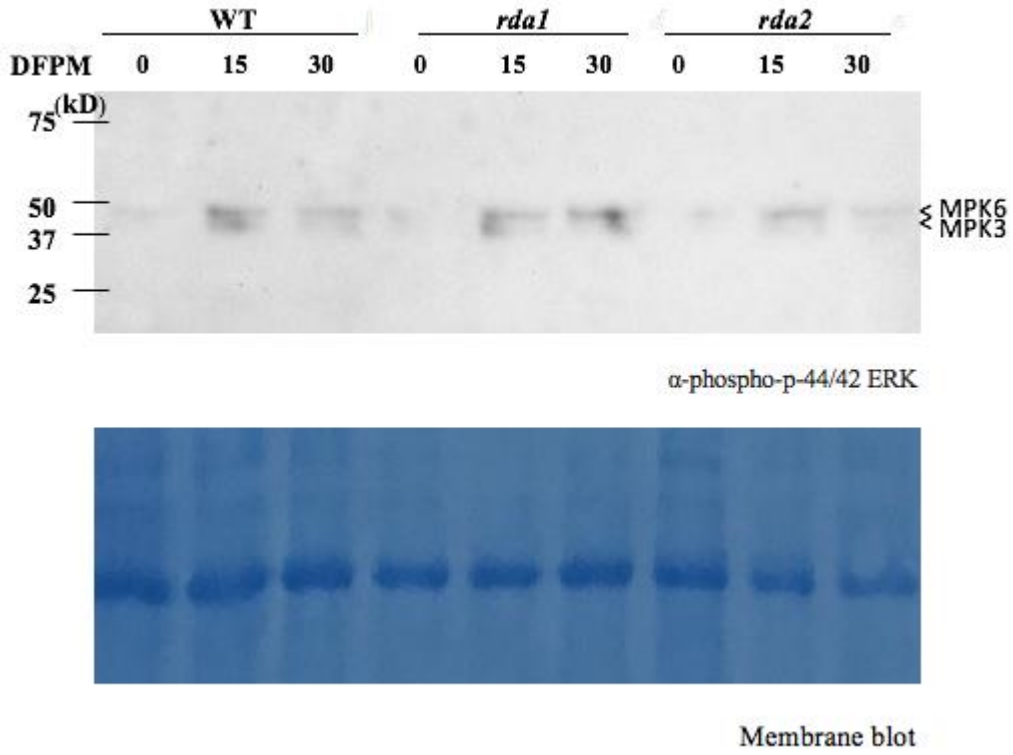

Figure 1.2: DFPM-mediated activation of MAP kinases in *rda1* and WT was examined in 14 day-old WT (Col-0 pRAB18::GFP), *rda1 pRAB18::GFP,* and *rda2 pRAB18::GFP* plants. Plants were treated with 30 μM DFPM for 0, 15, and 30 min(s) then whole proteins were extracted and blotted for. Phosphorylated MAP kinases were detected using anti-phospho-p44/42 MAPK (Erk1/2) (Thr202/Tyr204) antibody. *rda1 pRAB18::GFP* exhibited no clear evident difference to WT in DFPM-mediated activation of MAP kinases by marked arrowheads but shows an increased MPK 3 and MPK6 phosphorylation when compared to *rda2 pRAB18::GFP* (Park *et al.*, 2019). Loading controls: coomassie blue staining of membranes. Representative results from three independent repeats are shown.

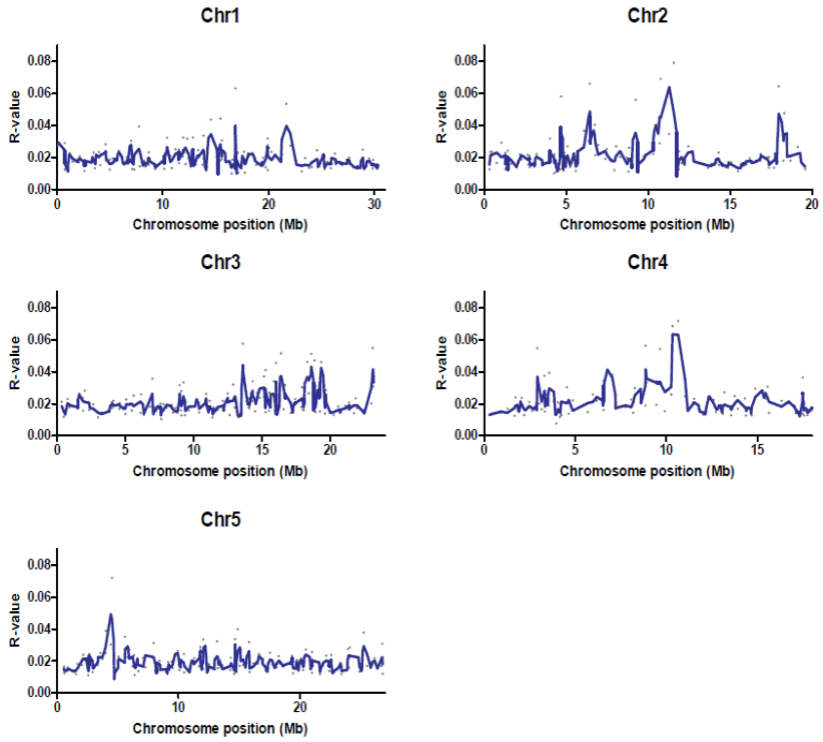

Figure 1.3: Bulk Segregant Analysis of *rda1* was completed via whole genome sequencing of 88 high confidence *rda1* mapping population BCF2 with highest quantified fluorescence of *RAB18::GFP* after DFPM followed by ABA treatment, in comparison to other *rda1 pRAB18::GFP* treated the same day. SNPs were identified by comparing *rda1* sequence with corresponding control Col-0 expressing *pRAB18::GFP*. R values of *rda1* specific SNPs for each base position were plotted on the five *A. thaliana* chromosomes (Benfey *et al*., 2017). Mapping population GFP fluorescence quantification and sequence analyses were completed by Jiyoung Park. MATLAB software was utilized in the generation of this figure.

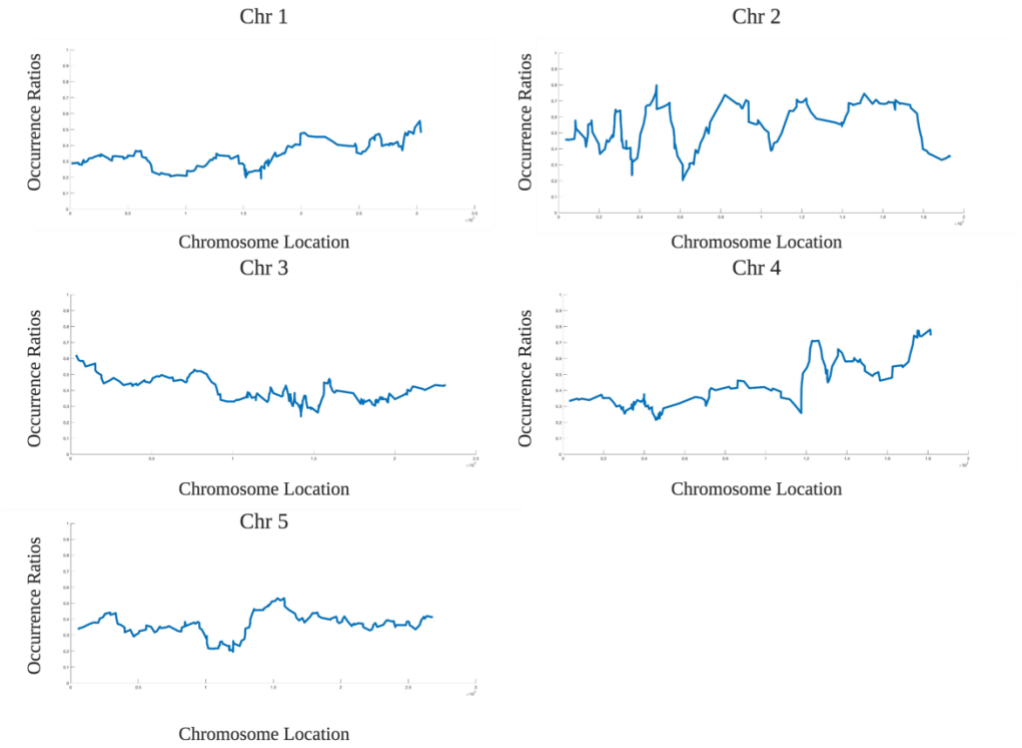

Figure 1.4: Bulk Segregant Analysis of *rda1* was completed via whole genome sequencing of high confidence *rda1* mapping population BCF3 with highest quantified fluorescence of *RAB18::GFP* area after DFPM followed by ABA treatment. 85 million reads were completed for this pooled genomic DNA sample, approximately 40X coverage of the *A. thaliana* genome. SNPs were identified by comparing *rda1* sequence with corresponding control Col-0 expressing *pRAB18::GFP*. Occurrence ratios of *rda1* specific SNPs for each base position were plotted on the five *A. thaliana* chromosomes (Benfey *et al*., 2017). Mapping population GFP fluorescence quantification and plots were generated via Jiyoung Park, genome analysis completed in the Glass lab by Sascha Duttke, genome sequence analysis was conducted with help from Jiyoung Park and Po-Kai Hsu.

Table 1.1: Logic and Algorithm to Identification of Candidate Causative Mutants

Whole genome sequencing results were analyzed via plotting of mutant occurrence ratios, isolation of EMS-type Single Nucleotide Polymorphisms (SNP), and identification of effective mutations. First, mutant occurrence ratios were plotted for each base position by identifying a value of ($ratio = \frac{wt_{ref}}{wt_{ref}+wt_{alt}} - \frac{mut_{ref}}{mut_{ref}+mut_{alt}}$). After the determination of peaks across the entirety of the *A. thaliana* genome, EMS-type SNPs were identified by choosing for mutations in the mutant sequence where base pairs cytosine and guanine were altered to thymine and adenine, respectively. Following, effective mutations which lead to missense, variation, or nonsense mutations were selected for. Lastly, the mutants with the highest occurrence ratios (>0.8) were selected for and chosen for further analysis via T-DNA insertion mutants.

Purpose	Action	Result
Plot Mutant read ratio	$ratio = \frac{wt_{ref}}{wt_{ref} + wt_{alt}} - \frac{mut_{ref}}{mut_{ref} + mut_{alt}}$	Determined occurrence ratio for each base position
Isolate EMS type SNP	Select for C to T and G to A - type mutation	881 mutations
Isolate Effective Mutations	Select for Missense / Variation / Nonsense mutations	Approximately 30 effective mutations per chromosome
Chromosome/ Gene Selection	Select for occurrence ratio > 0.8 to reduce false positives	9 possible causative mutations in chromosome 2, and 4 in chromosome 4

Table 1.2: *rda1* candidates were identified by following the logics described in **Table 1.1** using Matlab and Excel. Tables A contains the 9 candidates from *A.thaliana* chromosome 2, and Table B contains the 4 candidates from chromosome 4; candidates are listed in order of mutant read ratio with a variety of genes ranging from characterized to unknown functioning genes. Identification of causative mutants was found with help from Jiyoung Park.

A

Mutation	Gene name	At_num	CDS_change	protein_change	Mut ratio	Function
missense_variant	NLP1	AT2G17150	319G>A	Gly107Arg	0.944	Plant regulator RWP-RK family protein
early stop	ERD7	AT2G17840	845G>A	Trp282*	0.909	Early-responsive to dehydration 7
missense_variant	NCRK	AT2G28250	1315C>T	Arg439Trp	0.904	Protein kinase superfamily protein
missense_variant	ANN4	AT2G38750	661G>A	Asp221Asn	0.882	calcium dependent membrane binding protein
missense_variant	Unnamed	AT2G27460	41C>T	Ser14Leu	0.866	Sec23 homolog
missense_variant	Unnamed	AT2G02026	176C>T	Ala59Val	0.857	Unknown Function
missense_variant	Unnamed	AT2G13350	388G>A	Gly130Arg	0.857	Unknown Function
missense_variant	FBL10	AT2G17020	577G>A	Val193Ile	0.838	F-box/RNI-like superfamily protein;(source:Araport11)
missense_variant	RKP	AT2G22010	2927G>A	Gly976Glu	0.833	RING E3 ubiquitin ligase homolog

Table 1.2: Continued
B

Mutation	Gene	At_num	CDS_change	protein_change	Mut Ratio	Function
missense_variant	Unnamed	AT4G24810	827G>A	Gly276Asp	1	Protein kinase super family
stop_gained	NUP58	AT4G37130	187C>T	Gln63*	1	Member of the Nup62 subcomplex of the Arabidopsis NPC.
missense_variant	PCMP-H27	AT4G35130	445G>A	Gly149Arg	0.894	Tetratricopeptide repeat (TPR)-like superfamily protein
missense_variant	CRK12	AT4G23200	1541G>A	Gly514Asp	0.812	Cysteine-rich receptor-like protein kinase.

Col-0 pRAB18::GFP *rda1 pRAB18::GFP*

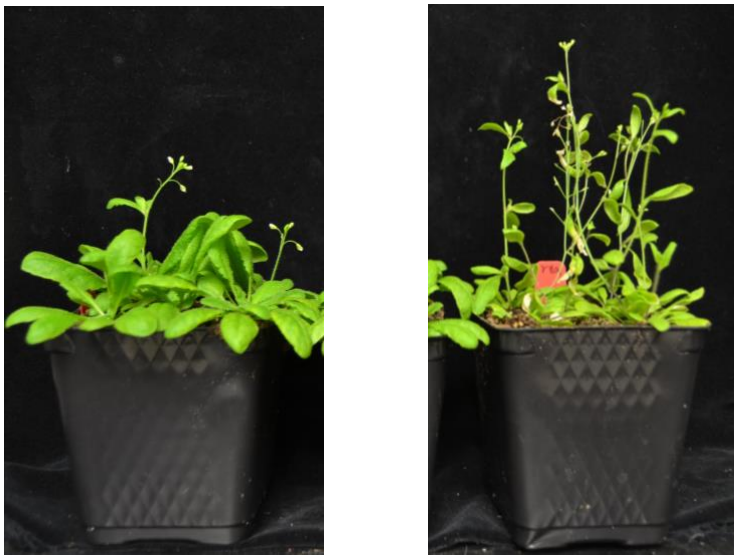

Figure 1.5 BC1F2 *rda1 pRAB18::GFP* demonstrates a growth phenotype in addition to the resistant to DFPM inhibition of ABA phenotype. *rda1 pRAB18::GFP* on the right side demonstrates a stunted size in growth and an early flowering phenotype, in comparison to the *Col-0 pRAB18::GFP* on the left hand side. These plants are both 40 days old at the time of capture, and is representative of the total population of *rda1 pRAB18::GFP* and Col-0 pRAB18::GFP utilized.

1.4 Discussion

Previous chemical genetics screening identified a small molecule, DFPM, that activates plant immune signaling transduction while inhibiting ABA signaling in a EDS1, PAD4, SGT1b, and RAR-1 dependent manner (Kim *et al.*, 2011, Kim *et al*., 2012, Park et al., 2019). DFPM was also further identified to induce root growth arrest in an ETI-mediated manner (Kunz *et al.*, 2016) further the DFPM bioactivity is light sensitive . To understand the molecular bases underlying DFPM inhibition of ABA signaling and DFPM-induced root growth arrest, we set out to conduct a forward genetics screen to identify new mutants insensitive to these phenotypes.

By a forward chemical genetics screen of EMS-mutagenized wild type Col-0 lines expressing ABA-mediating pRAB18::GFP promoter, *rda* mutants were isolated for its Resistant to DFPM inhibition of ABA (rda) phenotype when plants were pretreated with DFPM 1 hour prior to ABA treatment. Originally, 3 different *rda* mutants were isolated (*rda1, rda2,* and *rda3*) for its resistant to DFPM inhibition phenotype via changes in stomatal aperture. *Rda2* contained the strongest insensitivity to DFPM inhibition of ABA and was recently published as encoding for a lectin receptor kinase (Park *et al.*, 2019). *Rda1* and *Rda3,* on the other hand, have yet to be mapped to a causative mutation.

Here we demonstrate the resistance to DFPM inhibition of ABA phenotype in *rda1 pRAB18::GFP* and *rda2 pRAB18::GFP* via fluorescence microscopy (Figure 1.1). Although the *rda1 pRAB18::GFP* resistant to DFPM inhibition of ABA phenotype is not as strong as *rda2 pRAB18::GFP* (Figure 1.1), the current stock of *rda1 pRAB18::GFP* may still contain other EMS mutations, in contrast to *rda2 pRAB18::GFP* which is a T-DNA insertion mutant line. Additionally, this method of microscopy imaging was not the original method of identification for the *rda* mutants (Park et al, 2019). The original 3 resistant-to-DFPM inhibition of ABA

phenotypes were isolated via 96 well plate fluorescent imaging whereas currently we are analyzing fluorescence from abaxial surface epidermal pavement cells. There may exist technical or biological variance due to stomatal fluorescence and locations of images taken. These experiments should be repeated after isolating the causative mutation of *rda1* by repeating stomatal aperture analyses in addition to fluorescence microscopy.

In the meantime, we also investigated *rda1 pRAB18::GFP* phenotype in DFPM-induced phosphorylation of mitogen-activated proteins 3 and 6 (MPK3/6). Previously, experiments with *rda2 pRAB18::GFP* demonstrated a reduced MPK3/6 phosphorylation in comparison to Col-0 pRAB18::GFP in an ETI-signaling component non-required manner (Park et al., 2019). The reduction in MPK3/6 phosphorylation specific to *rda2* lectin receptor kinase knock out suggests that DFPM not only signals in an ETI-mediated manner via EDS1/PAD4/STG1b/RAR1 but possibly through an additional signal transduction pathway either downstream of or parallel to ETI-signaling components (Kim *et al.*, 2012, Kunz *et al.*, 2016, Park *et al.*, 2019). By testing *rda1* phenotype for DFPM-induced phosphorylation of MPK3/6, we found that *rda1*, when treated with DFPM chemical, leads to an increased MPK3/6 phosphorylation signal compared to *rda2* (Figure 1.2). In fact, *rda1* mutant MPK3/6 phosphorylation phenotype is WT-like, similar to previously published *eds1, pad4, sgt1b, rar1,* and *victr* phenotypes (Figure 1.2) (Park *et al.*,2019). Since MPK3 and MPK6 phosphorylation are early signal transduction components in drought tolerance, salt stress tolerance, and pathogen signaling (Jagodzik *et al.*, 2018; Park *et al.*, 2019), it is likely that *rda1* is different from *rda2* such that rda1 functions either downstream of or separate from DFPM-induced MPK/6 phosphorylation, like the ETI signaling components of EDS1, PAD4, SGT1b, RAR1, and VICTR.

Before further functional characterization of *rda1*, we decided to repeat previous efforts of mapping the *rda1* mutation. Previously, bulk segregant analysis was conducted for *rda1* utilizing 88 BC1F2 plants demonstrating strongest resistant to DFPM inhibition of ABA phenotype per pRAB18::GFP fluorescence imaging results (Figure 1.3). However, the Whole Genome Sequence based mapping attempt did not result in a clear peak like the *rda2* mutant despite the identical screening and sequencing methods by Dr. Park (Park *et al*., 2019). The *rda1* sequencing results yielded two or more small peaks and it was concluded that some wild-type plants had contaminated the mapping population (Figure 1.3). Therefore, attempting bulk segregant analysis again, we grew the BC1F3 generation and re-screened for a resistant to DFPM inhibition of ABA phenotype by isolating plants that demonstrated *rda*-like fluorescence in the epidermal pavement cells. Out of 73 plants, 11 demonstrated consistent *rda* fluorescence and were pooled for whole genome sequencing. Fortunately, the sequencing results indicated peaks at 2 separate chromosomes, however it is still not clear-cut like *rda2* (Figure 1.4) (Park *et al.,* 2019).

Following the bulk-segregant sequencing results, we ordered T-DNA insertion mutants for each of the 14 candidate mutants identified via the SIMPLE pipeline (Table 1.2) (Benfey *et al.,* 2017). Homozygous mutants were isolated for lines targeting the three mutants with the highest mutation occurrence ratio. We attempted to cross the multiple lines of homozygous mutants of each T-DNA insertion line with *rda1 pRAB18::GFP* and were unsuccessful. During growth and crossing, we noticed *rda1 pRAB18::GFP* demonstrated a stunted size in growth and an early flowering phenotype (Figure 1.5). Especially during crossing, we found *rda1* to contain very little pollen for plant-crossing, and the experiments were delayed. To note, however, *rda1 pRAB18::GFP* was previously backcrossed to its parental line Col-0 pRAB18::GFP; therefore, it

is also likely to be due to inexperience and technical error. Further crossing attempts will be carried out in the future for the candidate mutants (Table 1.2) with *rda1 pRAB18::GFP* to test for allelism in each homozygous T-DNA insertion mutant.

In summary, research was conducted to continue prior attempt of mapping the *rda1* mutation via repeated bulk segregant analysis. However, there is still space for improving sequencing results as there are more than 1 peak when analyzing occurrence ratios of possible causative SNPs in the *rda1 pRAB18::GFP* genome (Figure 1.3). Due to the small amount of plants utilized for the BC1F3 bulk segregant analysis, we believe there is limited resolution in the analysis provided. Since only 11 plants out of the original 73 BC1F3 plants demonstrated a resistance to DFPM inhibition of ABA signaling phenotype, there may be more contamination in the rda1 pool utilized and the phenotype should be confirmed in the seed pool. Future experiments should involve a repeated back-cross of *rd1 pRAB18::GFP* into parental Col-0 pRAB18::GFP line to increase purity of *rda1* phenotypes in sequencing pool, in addition to furthering the progenies of currently isolated *rda1 pRAB18::GFP*. We believe identification and proper mapping of *rda1* remains priority before further functional characterization of the current *rda1* pool to avoid contamination in the derived dataset. Once the *rda1* causative mutation is identified, T-DNA insertion lines at the loci should be tested to confirm the phenotype. Depending on the function of the *RDA1* gene, further assays should be pursued to determine its role in the DFPM-inhibition of ABA signaling phenotype. As *rda2* has been mapped to a lectin-receptor kinase, it was determined that it likely plays a role in the recognition of pathogen associated molecular patterns in PTI signaling (Park *et al.*, 2019, Robert-Seilaniantz *et al.*, 2011). However, other components of DFPM signaling remain elusive and requires further characterization. Identifying *rda1* would provide insight into the method to which DFPM

activates immune signaling, immune signaling interfering with drought signaling, or drought signal repression mechanisms.

References

Asselbergh, B., Curvers, K., França, S. C., Audenaert, K., Vuylsteke, M., Van Breusegem, F., & Höfte, M. (2007). Resistance to Botrytis cinerea in sitiens, an abscisic acid-deficient tomato mutant, involves timely production of hydrogen peroxide and cell wall modifications in the epidermis. *Plant Physiology*, *144*(4), 1863–1877. https://doi.org/10.1104/pp.107.099226

Assmann, S. M. (2013, January). Natural variation in abiotic stress and climate change responses in Arabidopsis: Implications for twenty-first-century agriculture. *International Journal of Plant Sciences*. https://doi.org/10.1086/667798

Atkinson, N. J., & Urwin, P. E. (2012). The interaction of plant biotic and abiotic stresses: from genes to the field. *Journal of Experimental Botany*, *63*(10), 3523–3543. https://doi.org/10.1093/jxb/ers100

Audenaert, K., De Meyer, G. B., & Höfte, M. M. (2002). Abscisic acid determines basal susceptibility of tomato to Botrytis cinerea and suppresses salicylic acid-dependent signaling mechanisms. *Plant Physiology*, *128*(2), 491–501. https://doi.org/10.1104/pp.010605

Bostock, R. M. (2005). Signal Crosstalk and Induced Resistance: Straddling the Line Between Cost and Benefit. *Annual Review of Phytopathology*, *43*(1), 545–580. https://doi.org/10.1146/annurev.phyto.41.052002.095505

Choudhury, F. K., Rivero, R. M., Blumwald, E., & Mittler, R. (2017). Reactive oxygen species, abiotic stress and stress combination. *Plant Journal*, *90*(5), 856–867. https://doi.org/10.1111/tpj.13299

Coll, N. S., Epple, P., & Dangl, J. L. (2011, August). Programmed cell death in the plant immune system. *Cell Death and Differentiation*. https://doi.org/10.1038/cdd.2011.37

Cutler, S. R., Rodriguez, P. L., Finkelstein, R. R., & Abrams, S. R. (2010). Abscisic acid: emergence of a core signaling network. *Annual Review of Plant Biology*, *61*, 651–679. https://doi.org/10.1146/annurev-arplant-042809-112122

Deinlein, U., Stephan, A. B., Horie, T., Luo, W., Xu, G., & Schroeder, J. I. (2014). Plant salt-tolerance mechanisms. *Trends in Plant Science*. Elsevier Ltd. https://doi.org/10.1016/j.tplants.2014.02.001

Eliceiri, K., Schneider, C. A., Rasband, W. S., & Eliceiri, K. W. (2012). NIH Image to ImageJ : 25 years of image analysis HISTORICAL commentary NIH Image to ImageJ : 25 years of image analysis. *Nature Methods*, *9*(7), 671–675. https://doi.org/10.1038/nmeth.2089

Finkelstein, R. (2013). Abscisic Acid Synthesis and Response. *The Arabidopsis Book*, *11*, e0166. https://doi.org/10.1199/tab.0166

Finkelstein, R. R., Gampala, S. S. L., & Rock, C. D. (2002). Abscisic Acid Signaling in Seeds and Seedlings. *The Plant Cell* , 14–45. https://doi.org/10.1105/tpc.010441

Foyer, C. H., Rasool, B., Davey, J. W., & Hancock, R. D. (2016, March 1). Cross- Tolerance to biotic and abiotic stresses in plants: A focus on resistance to aphid infestation. *Journal of Experimental Botany*. Oxford University Press. https://doi.org/10.1093/jxb/erw079

Fujii, H., Verslues, P. E., & Zhu, J. K. (2007). Identification of two protein kinases required for abscisic acid regulation of seed germination, root growth, and gene expression in Arabidopsis. *Plant Cell*, *19*(2), 485–494. https://doi.org/10.1105/tpc.106.048538

Glazebrook, J. (2005). Contrasting mechanisms of defense against biotrophic and necrotrophic pathogens. *Annual Review of Phytopathology*, *43*, 205–227. https://doi.org/10.1146/annurev.phyto.43.040204.135923

Hauser, F., Li, Z., Waadt, R., & Schroeder, J. I. (2017, December 14). SnapShot: Abscisic Acid Signaling. *Cell*. Cell Press. https://doi.org/10.1016/j.cell.2017.11.045

Jagodzik, P., Tajdel-Zielinska, M., Ciesla, A., Marczak, M., & Ludwikow, A. (2018). Mitogen-activated protein kinase cascades in plant hormone signaling. *Frontiers in Plant Science*, *9*(October), 1–26. https://doi.org/10.3389/fpls.2018.01387

Jay, F., Vitel, M., Brioudes F., Louis, M., Knobloch, T., & Voinnet, O. (2019). Chemical enhancers of post-transcriptional gene-silencing in Arabidopsis. *RNA*, rna.068627.118. https://doi.org/10.1261/rna.068627.118

Kim, T.-H., Kunz, H.-H., Bhattacharjee, S., Hauser, F., Park, J., Engineer, C., Liu, A., Ha, T., Parker, J. E., Gassmann, W., Schroeder, J. I. (2012). Natural Variation in Small Molecule-Induced TIR-NB-LRR Signaling Induces Root Growth Arrest via EDS1- and PAD4-Complexed R Protein VICTR in Arabidopsis. *The Plant Cell*, *24*(12), 5177–5192. https://doi.org/10.1105/tpc.112.107235

Kim, T.-H., Böhmer, M., Hu, H., Nishimura, N., & Schroeder, J. I. (2010). Guard Cell Signal Transduction Network: Advances in Understanding Abscisic Acid, CO 2 , and Ca 2+ Signaling . *Annual Review of Plant Biology*, *61*(1), 561–591. https://doi.org/10.1146/annurev-arplant-042809-112226

Kim, T.-H., Hauser, F., Ha, T., Xue, S., Böhmer, M., Nishimura, N., Munemasa, S., Hubbard, K., Peine, N., Lee, B.H., Lee, S., Robert N., Parker, J.E., Schroeder, J. I. (2011). Chemical genetics reveals negative regulation of abscisic acid signaling by a plant immune response pathway. *Current Biology : CB*, *21*(11), 990–997. https://doi.org/10.1016/j.cub.2011.04.045

Knight, H., & Knight, M. R. (2001). Abiotic stress signalling pathways: Specificity and cross-talk. *Trends in Plant Science*. https://doi.org/10.1016/S1360-1385(01)01946-X

Kunz, H. H., Park, J., Mevers, E., García, A. V., Highhouse, S., Gerwick, W. H., Parker, J.E., Schroeder, J. I. (2016). Small molecule DFPM derivative-activated plant resistance protein signaling in roots is unaffected by EDS1 subcellular targeting signal and chemical genetic isolation of VICTR R-protein mutants. *PLoS ONE*, *11*(5), 1–20. https://doi.org/10.1371/journal.pone.0155937

Maekawa, T., Kufer, T. A., & Schulze-Lefert, P. (2011, September). NLR functions in plant and animal immune systems: So far and yet so close. *Nature Immunology*. https://doi.org/10.1038/ni.2083

Mittler, R. (2006). Abiotic stress, the field environment and stress combination. *Trends in Plant Science*, *11*(1), 15–19. https://doi.org/10.1016/j.tplants.2005.11.002

Nakashima, K., & Yamaguchi-Shinozaki, K. (2013, July). ABA signaling in stress-response and seed development. *Plant Cell Reports*. https://doi.org/10.1007/s00299-013-1418-1

Park, J., Kim, T. H., Takahashi, Y., Schwab, R., Dressano, K., Stephan, A. B., Ceciliato, P., Ramirez, E., Garin, V., Huffaker, A., Schroeder, J. I. (2019). Chemical genetic identification of a lectin receptor kinase that transduces immune responses and interferes with abscisic acid signaling. *Plant Journal*, 1–19. https://doi.org/10.1111/tpj.14232

Pastori, G. M., & Foyer, C. H. (2002). Common components, networks, and pathways of cross-tolerance to stress. The central role of "redox" and abscisic acid-mediated controls. *Plant Physiology*. https://doi.org/10.1104/pp.011021

Pieterse, C. M. J., Leon-Reyes, A., Van Der Ent, S., & Van Wees, S. C. M. (2009). Networking by small-molecule hormones in plant immunity. *Nature Chemical Biology*. Nature Publishing Group. https://doi.org/10.1038/nchembio.164

Robert-Seilaniantz, A., Grant, M., & Jones, J. D. G. (2011). Hormone crosstalk in plant disease and defense: more than just jasmonate-salicylate antagonism. *Annual Review of Phytopathology*, *49*, 317–343. https://doi.org/10.1146/annurev-phyto-073009-114447

Schneeberger, K., Ossowski, S., Lanz, C., Juul, T., Petersen, A. H., Nielsen, K. L., Jorgensen JE., Weigel D., Anderson S. U. (2009). SHOREmap: Simultaneous mapping and mutation identification by deep sequencing. *Nature Methods*. https://doi.org/10.1038/nmeth0809-550

Wachsman, G., Modliszewski, J. L., Valdes, M., & Benfey, P. N. (2017). A simple pipeline for mapping point mutations. *Plant Physiology*, *174*(3), 1307–1313. https://doi.org/10.1104/pp.17.00415

Zhang, X., Henriques, R., Lin, S. S., Niu, Q. W., & Chua, N. H. (2006). Agrobacterium-mediated transformation of Arabidopsis thaliana using the floral dip method. *Nature Protocols*, *1*(2), 641–646. https://doi.org/10.1038/nprot.2006.97

Chapter 2

Developing a Novel Chemical Genetics Screen to Identify Genetic Components Involved in DFPM-induced Root Growth Arrest

Abstract

A forward chemical genetics screen identified a small molecule DFPM, [5-(3,4-dichlorophenyl)furan-2-yl]-piperidine-1-ylmethanethione that triggers responses via *Arabidopsis thaliana* immune signaling transduction components, while inhibiting abscisic acid-signaling transduction. Beyond its role in this signal crosstalk, DFPM has also been found to induce root growth arrest in an Effector-Triggered-Immunity-dependent manner that is largely independent of abscisic acid. These phenotypes resulting from DFPM chemical treatment serve as an interesting platform for further elucidation of stress signaling crosstalk and pathogen-induced cell death signaling, two very complex and less understood pathways. Here I describe the development of a novel chemical genetics screening protocol designed to screen a large-scale artificial microRNA library to identify genetic families and redundancies in the *A. thaliana* genome that play a functional role in the DFPM-induced root growth arrest and possible cell death response. Seedlings containing artificial microRNA sequences targeting at least 2 genetically similar RNA/DNA binding proteins with possible off target mutations are utilized to assess for multi-gene knockdown mutants while having the advantage of versatile backtracking to identify the causative mutation without mapping or whole genome sequencing. Utilizing this screening protocol, we have confirmed 3 mutants that demonstrate a consistent resistance to DFPM-induced root growth arrest in at least 2 generations and continue to screen for and confirm more possible mutants.

2.1 Introduction

Given the difficulty I faced mapping *rda1*, we aimed to develop a screen in parallel to understand a known DFPM-induced response in *A. thaliana.* Beyond inhibiting drought- induced ABA signaling pathways, DFPM exposure also shows a root growth arrest in the accession Columbia-0 (Kim *et al.,* 2012, Kunz *et al.,* 2016). When roots were exposed to DFPM, the primary meristem of roots would form a hook and halt root growth. This root growth arrest phenotype can occur in both primary and lateral roots and was irreparable after transfer to control growth media together with other observations, demonstrating a likely cell death phenotype (Kim *et al.,* 2012).

Cell death responses, though common, are not well understood in plant systems due to the complex cross regulation between immune signaling pathways. Traditionally, cell death occurs due to the activation of defense responses following the perception of a specific pathogen effector signal (Glazebrook *et al.,* 2005, Hammond-Kosack and Jones, 1996). This effector signal-specific responses have been characterized with a gene-for-gene recognition of the intruding pathogen, also known as a gene-for-gene model (Flor, 1942, 1946).

The gene-for-gene model describes that for each gene encoding for resistance in the host organism, there is a corresponding gene to have coevolved encoding for avirulence in the pathogen that allows the host to perceive the avirulence product and mount an appropriate immune response (Flor, 1942, 1946). Therefore, only plants carrying the corresponding resistance genes specific for the complementing avirulence product can perceive and mediate the appropriate responses (Bakker *et al.,* 2006, Flor, 1942, 1946, Luderer *et al.,* Martin et al 2002, Richly *et al.,* 2002, Takken *et al.,* 2006). These specific resistance genes encode for resistance proteins which perceive the pathogen elicitor signals or facilitate downstream signal transduction

(Cohn *et al.,* 2001, Martin *et al.,* 2003, Meyers *et al.,* 2003, Takken and Joosten, 2000, Van de Weyer *et al.,* 2019).

Given that DFPM chemical treatment has been shown to elicit a root cell death-like response, we hypothesized that DFPM may in fact be perceived as a pathogen elicitor signal (Kim *et al.,* 2011, Kim *et al.,* 2012, Kunz *et al.,* 2016, Park *et al.,* 2019). However, knowledge in how DFPM is perceived and the downstream signaling pathways causing root growth arrest is still limited with gaps to fill in the signal transduction pathway.

Previously, we discovered that genetic variations in *Arabidopsis thaliana* accessions mapped to a Toll-IL-1 (TIR) - nucleotide binding (NB) - leucine-rich repeat (LRR) gene *VICTR* (VARIATION IN COMPOUND TRIGGERED ROOT growth response) locus disrupted the dramatic DFPM-induced root growth arrest (Kim *et al*, 2012, Kunz *et al.,* 2016). TIR-NB-LRR proteins are a subfamily of plant Nucleotide Binding Site (NBS) - leucine-rich repeat (LRR) resistance proteins hypothesized to be plant effector triggered immune receptors (McHale *et al.,* 2006; Martin *et al.,* 2003). Deriving from *victr* insensitivity to DFPM-induced root growth arrest, it was confirmed that DFPM may mimic an unidentified pathogen effector to activate VICTR - mediated signal transduction (Jones and Dangl, 2006; Dangl *et al.,* 2001; Kim *et al.,* 2012) and promote cell death signal transduction. Similar phenotypes have been found in the literature where a localized cell death response is activated in order to limit pathogen damage to the root growth(Glazebrook *et al.,* 2005); however, the signal transduction behind this DFPM-induced programmed cell death remain unclear.

Upon further experimentation, a similar resistance to DFPM-induced growth arrest was identified in effector-triggered immunity signaling components, *eds1, pad4, sgt1b,* and *rar1* mutants. In contrast, DFPM-induced root growth arrest phenotype continued in various jasmonic

acid signaling mutants and salicylic acid biosynthesis and signal transduction mutants (Kim *et al.,* 2012, Kunz *et al.,* 2016). Kim and colleagues demonstrated a clear morphological distinction between DFPM-induced root growth arrest and salicylic acid-induced root growth arrest, with contrasting root elongation, lateral root initiation, and root hair formation phenotypes (Kim *et al.,* 2012; Kunz *et al.,* 2016). The differences in phenotype between the effector-triggered immunity signaling mutants and the jasmonic and salicylic acid biosynthesis mutants suggests that DFPM indeed acts on an effector-triggered immunity specific pathway independent of salicylic acid and jasmonic acid disease signaling network in its induction of root growth arrest and root meristem death(Kim *et al.,* 2012).

Given the current *victr, eds1, pad4, rar1,* and *sgt1b* phenotypes in inhibition of DFPM-induced root growth arrest, it is hypothesized that DFPM-induced cell death response may be mediated by additional effector-triggered proteins and their functionally redundant homologs. In plants especially, a multitude of genes with highly similar sequences exist, leading to both genetic redundancy and functional overlap in gene function (Wagner 2015; Hauser *et al.,* 2013). With this understanding, we became interested in screening not for single-gene mutants, but higher order mutants accounting for this genetic redundancy in the *A. thaliana* genome.

To account for genetic redundancies, we utilized an artificial microRNA approach (Hauser *et al.,* 2019) to screen artificial microRNA lines containing individual artificial microRNAs designed to target and knockdown two or more homologous genes within subclades of *A. thaliana* transcription factors and protein kinase families. This approach allowed for specific targeting of diverse genetic combinations to capture robust phenotypes generated by homologous gene silencing (Hauser *et al.,* 2013; Hauser *et al.,* 2019). It has been validated and

utilized in recent publications to discover novel ABA, CO2, and auxin responsive mutants, confirming its potential to conduct comprehensive analysis of the functional overlap in the *A. thaliana* genome (Hauser *et al.,* 2013; Hauser *et al.,* 2019, Zhang *et al.,* 2018).

Here we developed a screening protocol to identify novel genetic components which likely facilitates DFPM-induced root growth arrest. Over 14,000 seeds have been screened for a resistance to DFPM-induced root growth arrest and 77 mutants have been isolated, with 3 so far showing a repeated phenotype in at least two generations.

2.2 Materials and Methods

Pooled Screen Plant Material and Growth Conditions

Artificial microRNA-transformed seeds and controls (Col-0 expressing artificial microRNAs targeting human myosin2 and *victr*) seeds were surface sterilized with 10% bleach for 10 minutes, rinsed with sterile water five times, then placed in the dark at 4 °C for 48 hours for cold treatment before transfer to a 16/8h light/dark growth chamber at 21 °C for 24 hours. Seeds were then plated onto ½ Murashige and Skoog, 1% sucrose, and 0.8% agar, pH 5.8 media containing and 10 µM DFPM and wrapped with aluminum foil and grown vertically in a 16/8h light/dark growth chamber at 21 °C for 7 days. On day 8, the plates were uncovered from aluminum foil and lengths of root growth were demarcated. Plates were placed back into the 16/8h light/dark growth chamber at 21 °C for 5 days. On day 11-13, the artificial microRNA-expressing seedlings with sustained root growth and control (*col-0*) seeds were transferred to ½ Murashige and Skoog, 0.8% agar, pH 5.8 plates containing 50 µM Glufosinate ammonium (BASTA) and grown in a 16/8 light/dark growth chamber at 21 °C for 7 days.

Confirmation Screen Plant Material and Growth Conditions

Artificial MicroRNA seedlings with controls (Col-0 with artificial microRNA targeting human myosin 2) were surface sterilized with 10% bleach for 10 minutes, rinsed with sterile water five times, plated onto ½ Murashige and Skoog, 1% sucrose, and 0.8% agar, pH 5.8 media and placed in 4 °C for 48 hours for cold treatment before transfer to a 16/8h light/dark growth chamber at 21 °C for 8 days of vertical growth. On day 9, the seedlings were transferred to ½ Murashige and Skoog, 1% sucrose, and 0.8% agar, pH 5.8 media containing 10 µM DFPM, with

aligned seedling root tips and grown vertically in 16/8h light/dark growth chamber at 21 °C for 8 days.

Selection of Artificial MicroRNA Construct

To confirm artificial microRNA constructs within mutant plants, each mutant phenotype seedling was exposed to BASTA antibiotic for artificial microRNA transformed line selection. In both the pooled artificial microRNA screening protocol, control seeds and mutant phenotype candidate seeds were transferred to ½ Murashige and Skoog plates containing 50 µM Glufosinate Ammonium (BASTA) and grown for 5-7 days.

2.3 Results

DFPM was a chemical found via a chemical library screen to inhibit ABA signal transduction and induce root growth arrest after DFPM treatment (Kim *et al.*, 2011, Kim et al., 2012). Upon exposure to DFPM, primary roots of wild-type seedlings formed a hook and halted its growth (Figure 2.3 A, Figure 2.3 C). To dissect the genetic components involved in this DFPM-induced cell death response, we developed a protocol (Figure 2.1) to screen for large amounts of mutant seeds for the DFPM-induced root growth arrest phenotype.

Pooled Artificial MicroRNA Mutant Screen Development

This first protocol (Figure 2.1 A) was developed specifically for the pooled artificial microRNA mutant library screen. Previous studies grew seeds on regular media before physical transfer onto a DFPM-containing media (Kunz *et al.,* 2016). This method, while least confounding to isolate a DFPM-effect, was very labor intensive and prone to bacterial or fungal contamination when attempted with large-scale screening. Not only was it inefficient in the amount of time required to transfer individual seedlings by hand onto a new plate, but it also risked the validity of the root growth arrest phenotype when any contamination occurred. To reduce the labor requirement and likelihood of contamination, a new protocol was developed to grow the artificial microRNA mutant seeds directly onto DFPM containing growth media after vernalization and light treatment.

However, a second problem was the decreasing bioactivity of the DFPM chemical once exposed to light. DFPM is light sensitive and its bioactivity degrades over a 24h period after light exposure (Kunz *et al.,* 2016). During the pilot stages of this protocol development, we

attempted growing seedlings on DFPM-containing media, exposed to light. However, when examining the root length phenotypes of the seedlings on DFPM, it was evident that most artificial microRNA mutants including negative control wild type seeds did not display a DFPM-induced root growth arrest phenotype, suggesting that DFPM had lost its bioactivity after 5 days under light exposure, as can be expected (Kunz et al., 2016). However, we maintained the idea where seeds were to be plated directly on DFPM-containing plates to increase screening efficiency. Therefore, to prevent bioactivity degradation and ensure DFPM inhibition effect on root development, DFPM-containing plates were wrapped in aluminum foil directly after seed placement and then grown in a vertical position(70-80°) while wrapped.

After growth in DFPM containing media, a third problem existed where mutant root growth was commonly delayed in the screening pool. Traditionally, seeds are grown for 3 to 4 days before exposure to a chemical treatment. However, in this case, at 4 days it was found that mutant seedling growth showed a spectrum ranging from not germinated to minimal primary root development in comparison to control seedlings with visible primary root development. In fact, in the case when the primary roots were not properly developed in the pilot screen prior to light activation of DFPM bioactivity, a large number of false positives occurred where seedlings that were not resistant to DFPM-inhibition of root growth arrest would continue root growth on DFPM-containing media possibly because the roots were not developed at the time of light activation of DFPM activity. Therefore, seeds grown on DFPM containing plates were covered for 7 days before removal of aluminum foil wrapping to allow for proper mutant root growth prior to light activation of DFPM.

At day 8, root lengths were demarcated on each plate and then placed into growth chambers for 16/8h light/dark vertical (70-80°) growth, this time exposed to the light and activating DFPM inhibition of root growth activity. After 5 more days, continued growth of the primary roots' tip locations were marked again in a different color, often under a microscope, to confirm the continued growth of primary roots instead of lateral roots. The artificial microRNA lines which exhibited a resistance to DFPM-induced root growth arrest were then transferred to BASTA antibiotic-containing growth media to select for the amiRNA-expression lines within the mutants for 5 days, with Col-0 (negative control for BASTA selection) for comparison. After 7 days, if the plants grew successfully, they were then transferred to regular soil growth for maturation and seed collection and future generational testing.

Confirmation of Artificial MicroRNA Mutant Screen Development

The second protocol (Figure 2.1 B) was developed for the confirmation of mutant seeds derived from isolated mutants of the first protocol (Figure 2.1 A). This protocol is a similar but shortened version of the method utilized in (Kim *et al.,* 2012). Instead of vertical growth for 10 days, the time was decreased to 7 days without leading to increased false-positive mutants. After 7 days of growth on standard growth media, seedlings were transferred to DFPM-containing growth media for a DFPM-induced root growth assay. Due to the significantly decreased amount of seeds screened in this candidate confirming protocol, this trade off of mutant validation for labor efficiency was deemed appropriate while also accounting for any skotomorphogenesis confounds in the pooled artificial microRNA screening protocol. If there were root growth differences due to the primary roots grown in the dark, the confirmation screen of roots grown in the light prior to DFPM treatment would eliminate any phenotypes and isolate only phenotypes

due to growth on DFPM-containing media. On day 8, the successfully grown mutants were then transferred to regular soil growth for maturation and seed collection and future generational testing. BASTA antibiotic was applied to these plants via spray during maturation on soil.

Screening Progress

Thus far, approximately 14,000 seeds from the artificial microRNA transcription factor and RNA/DNA binding protein pool were screened on DFPM media for root growth arrest (Figure 2.2). A total of 92 microRNA mutants showed a resistant to DFPM-induced root growth arrest phenotype and were selected for BASTA resistance testing (Figure 2.1 A). Within the 92 mutants collected and grown in soil, 15 of 92 failed to mature to seed production. The other 77 of 92 were successfully grown and subjected to the secondary screening (Figure 2.1B, Figure 2.2). Of the 77 successfully grown mutants that were impaired in the DFPM-induced root growth arrest, 19 of 77 mutants did not show a clear repeat in DFPM-induced root growth arrest. 53 of 77 mutants have yet to be tested, and 3 of 77 have been isolated that show a repeated resistance to DFPM-induced root growth arrest phenotype and also contain an amiRNA construct based on BASTA antibiotic resistance selection.

Isolated Mutant Candidates with Repeat Phenotypes

The 3 mutants isolated for their repeated resistance to DFPM-induced root growth arrest were grown and labeled as Artificial MicroRNA (AmiRNA) Mutant 11, 12, and 24. These numbers were assigned given the order of which they were isolated. The mutants isolated before and between them either did not demonstrate a repeat in mutant phenotype of root growth

continuation on DFPM containing media or did not survive BASTA antibiotic selection (Figure 2.3 B).

AmiRNA Mutant 11 was the first mutant isolated with a repeat in phenotype. T3 seeds were subjected to the confirmation screen (Figure 2.1 B) in parallel with control seeds of Col-0 expressing artificial microRNA targeting human myosin 2 (amiRNA-HsMyo), which targets no genes in *A. thaliana* (Hauser *et al.,* 2013). After transfer to DFPM containing growth media for 4 days, amiRNA mutant 11 continued to demonstrate root growth, contrasting control seeds (Figure 2.4 A). The root lengths of AmiRNA mutant 11 in Figure 2.4 A were quantified via segmental measuring tool within ImageJ software (Elicieri *et al.,* 2017) and plotted in Figure 2.4 B. AmiRNA Mutant 11 T3 root lengths demonstrate a significant increase contrasting control (amiRNA-HsMyo) root lengths after transfer to DFPM growth media. The differences in root lengths were deemed significant via 1-way ANOVA test with p value <0.00001.

Following the repetition in phenotype, the amiRNA mutant 11 was sequenced to identify the artificial microRNA construct target. The artificial microRNA construct was found to contain sequence TCATTCGCCAAACTTCGGCA, which corresponds to the gene loci At5g63270 and At2g04410 according to the PHANTOM library (Table 2.1; Hauser *et al.,* 2013; Hauser *et al.,* 2019). These two genes correspond to two separate Resistant to *Pseudomonas syringa*e pv *maculicola 1* (RPM1)- interacting protein 4 (RIN4) family members (Figure 2.5). The genetic sequence of the two family proteins were aligned with the various RIN4-related homologs and the original RIN4 (**ad Ag #s) to generate a phylogenetic tree (Figure 2.5).

Although the two genes targeted by AmiRNA mutant 11 have not been characterized in the literature yet, a related gene product RIN4 has been described in the literature as a protein that is phosphorylated upon infection by *P. syringae* expressing AvrB or AvrRpm1 and leads to

activation of RPM1, a Coiled-coiled (CC) - Nucleotide-Binding (NB) - Leucine Rich Repeat (LRR) Resistant protein, and RPM1-mediated disease resistance (Mackey *et al.,* 2002). Additionally, RIN4 has also been published to negatively regulate Resistance to *P. syringae 2* (RPS2), another Nucleotide-Binding (NB) - Leucine-Rich Repeat (LRR) protein (Mackey *et al.,* 2003). Both of these NB-LRR gene-encoding proteins that interact with RIN4 have been published to be involved in the detection and/or defense to *P. syringae* with different avirulent factors. Interestingly, both of these downstream elements been previously tested to be unnecessary for DFPM-induced root growth arrest (Kunz *et al.,* 2016).

In addition to AmiRNA mutant 11, amiRNA mutants 12 and 24 both showed a repeat in resistance to DFPM-induced root growth arrest in the confirmation screening protocol as well (Figure 2.1 B). AmiRNA mutant 12 T3 and AmiRNA mutant 24 T4-1 seeds were subjected to the confirmation screen (Figure 2.1 B) in parallel with control (amiRNA-HsMyo) (Hauser *et al.,* 2013). After transfer to DFPM-containing growth media for 8 days, AmiRNA mutant 12 and 24 both showed continuous root growth, contrasting control seeds (Figure 2.7 A, Figure 2.8 A). The root lengths of the AmiRNA mutants 12 and 24 were quantified via the segmental measuring tool of ImageJ software(Elicieri *et al.,* 2017) and plotted in Figures 2.7 B and Figure 2.8 B, respectively. Both AmiRNA Mutant 12 T3 and Mutant 24 T4-1 root lengths demonstrate a significant difference from control root lengths after transfer to growth media. The differences in root lengths were deemed significant via 1-way ANOVA test with p value <0.00001.

Contrasting amiRNA mutant 11, however, amiRNA mutants 12 and 24 require sequencing to identify the gene targets of the contained artificial microRNA constructs. Each of these isolated mutants may provide insight into additional genetic components possibly required for DFPM-induced root growth arrest. Based on the repeated phenotype in amiRNA mutants 11,

12, and 24 so far, it is likely that the genes which are silenced in each line play a critical role in wild-type DFPM-induced root growth arrest.

Figure 2.1 Screening Protocol developed for Root Growth Arrest Screen: (A) Pooled Artificial MicroRNA Screening, and (B) Confirmation Screen of Mutant Candidates

A. Pooled amiRNA seeds are grown on ½ Murashige and Skoog, 1% sucrose, and 0.8% agar plates containing 10µM DFPM along with control seeds. Plates are covered in aluminum foil and grown vertically. On day 7, aluminum foil is removed, and root length development is marked on the plates. On day 11, the root length development is remarked in a different color. Seedlings with root growth after the first demarcation is then transferred to BASTA-containing plates for selection with control seedlings. On day 15-18, BASTA-resistant seedlings are then transferred to soil for mature development.

B. AmiRNA mutant seeds and control seeds are grown directly on regular ½ Murashige and Skoog, 1% sucrose, and 0.8% agar plate for vertical growth. On day 8, seedlings are transferred to DFPM-containing ½ Murashige and Skoog, 1% sucrose, and 0.8% agar plates with tip of root length placed onto standard line for vertical growth. After 5-9 days, images are taken of root length development. Successful mutants are transferred to soil and subjected to BASTA selection via spray during maturation.

A

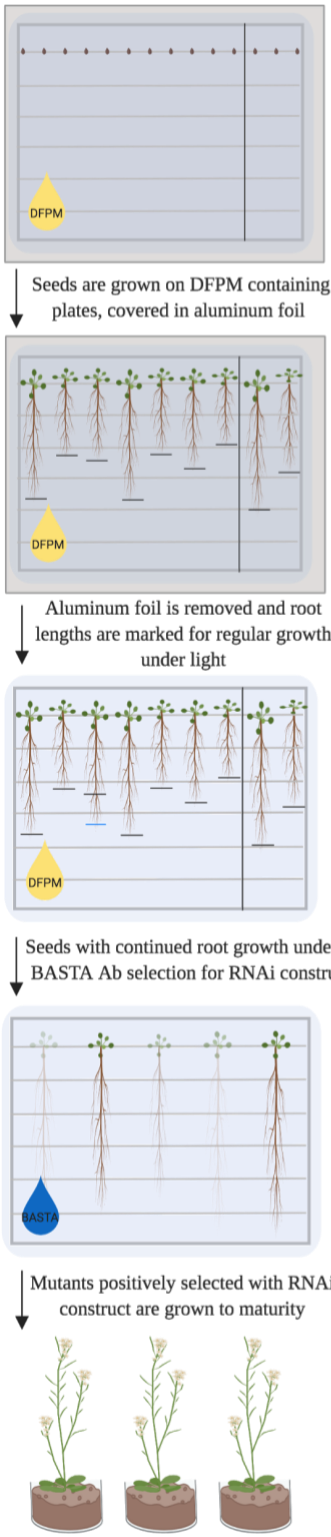
DFPM
Seeds are grown on DFPM containing plates, covered in aluminum foil
DFPM
Aluminum foil is removed and root lengths are marked for regular growth under light
DFPM
Seeds with continued root growth undergo BASTA Ab selection for RNAi construct
BASTA
Mutants positively selected with RNAi construct are grown to maturity

B

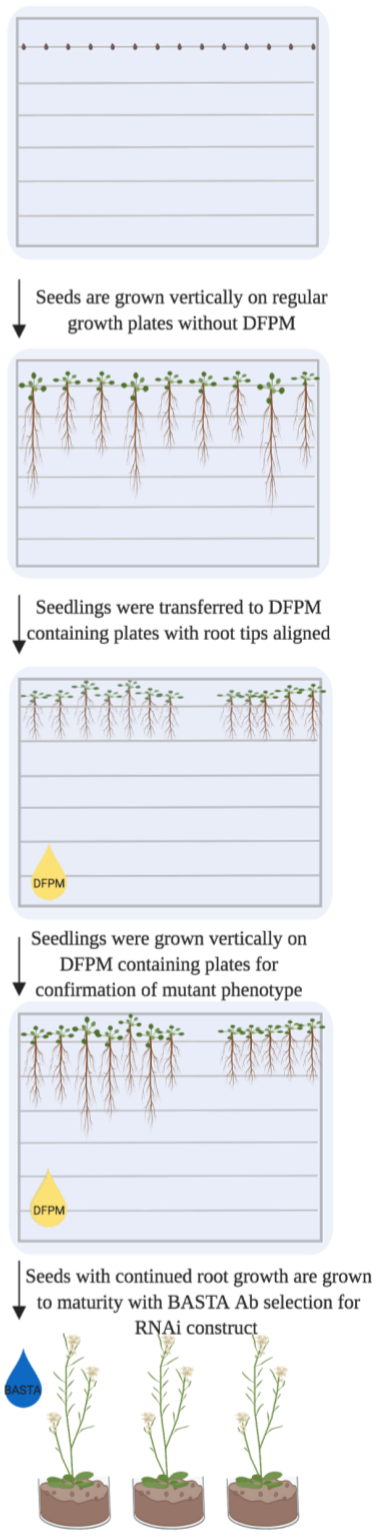
Seeds are grown vertically on regular growth plates without DFPM
Seedlings were transferred to DFPM containing plates with root tips aligned
DFPM
Seedlings were grown vertically on DFPM containing plates for confirmation of mutant phenotype
DFPM
Seeds with continued root growth are grown to maturity with BASTA Ab selection for RNAi construct
BASTA

Figure 2.2 Total Screening Progress

Out of the total pool of artificial microRNA mutants targeting the transcription factors and DNA/RNA binding proteins (TFB), 14,212 seeds have been screened. 92 out of 14,212 were found to be resistant to DFPM-induced Root Growth Arrest and contained the RNAi construct via BASTA antibiotic selection. 77 out of the 92 have successfully grown and are yielding seeds to be tested in the next generations. 3 out of 77 successfully grown have been found to repeat the mutant resistant to DFPM-induced root growth arrest phenotype thus far.

Pooled TFB Artificial MicroRNA Mutant Library

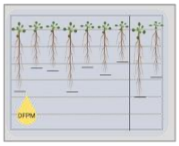

14, 212 seeds screened for DFPM-induced Root Growth Arrest

14,097 mutants exhibited WT phenotype of DFPM-induced root growth arrest or were BASTA-sensitive

92 mutants resistant to DFPM-induced Root Growth Arrest and BASTA-resistant

15 lines did not grow to maturity to produce seeds for future generation testing

77 successfully growing mutants yielding seeds for DFPM root growth arrest assay in the T3 generation

53 mutants untested for repeat phenotype in DFPM-induced root growth arrest assay

19 mutants did not repeat resistance to DFPM-induced root growth arrest phenotype

3 artificial microRNA mutant repeated resistant to DFPM-induced Root Growth Arrest

Figure 2.3 Seedling Growth Responses during Screening Process is as follows:

A) Images were taken from the pooled artificial microRNA screening protocol (Figure 2.1 A). Seeds were grown on ½ Murashige and Skoog, 1% sucrose, 0.08% agar, and 10 µM DFPM media containing plates, wrapped in aluminum foil for 7 days. Then, plates were unwrapped and root lengths were marked in blue and left to grow vertically for 5 more days. These images were taken after 5 days of growth under DFPM-activated light conditions. The left bottom image refers to an example of a mutant which exhibited resistance to DFPM-induced root growth arrest. The bottom right image refers to an example on the same growth plate that did not exhibit resistance to DFPM-induced root growth arrest.
B) Images were taken from the BASTA Antibiotic screening step of the pooled microRNA screening protocol (Figure 2.1 A). Seedlings which exhibited resistance to DFPM-induced root growth arrest were selected for and transferred onto a 50 µM Glufosinate Ammonium (BASTA) containing ½ Murashige and Skoog, 0.08% agar plate. Images were taken after 5 days of exposure to BASTA antibiotic. The left bottom image refers to an example of a mutant which survived BASTA antibiotic, the bottom right refers to a mutant from the same plate that did not survive BASTA antibiotic.
C) Images were taken from the confirmation screening experiment following protocol described in Figure 2.1B. Seedlings were transferred from ½ Murashige and Skoog, 1% sucrose, 0.08% agar medium after 8 days of growth and were transferred to 10 µM DFPM media containing ½ Murashige and Skoog, 1% sucrose, 0.08% agar plates for growth. These images were taken after 8 days of growth on DFPM. The left bottom image refers to an example of a mutant which exhibited a repeated resistance to DFPM-induced root growth arrest, and the bottom right refers to the control (amiRNA-HsMyo) which do not exhibit resistance to DFPM-induced root growth arrest. In the left image, there is continued growth of the primary root on DFPM-containing media after the alignment, whereas in the right image the primary root has arrested and lateral roots have begun growing instead.

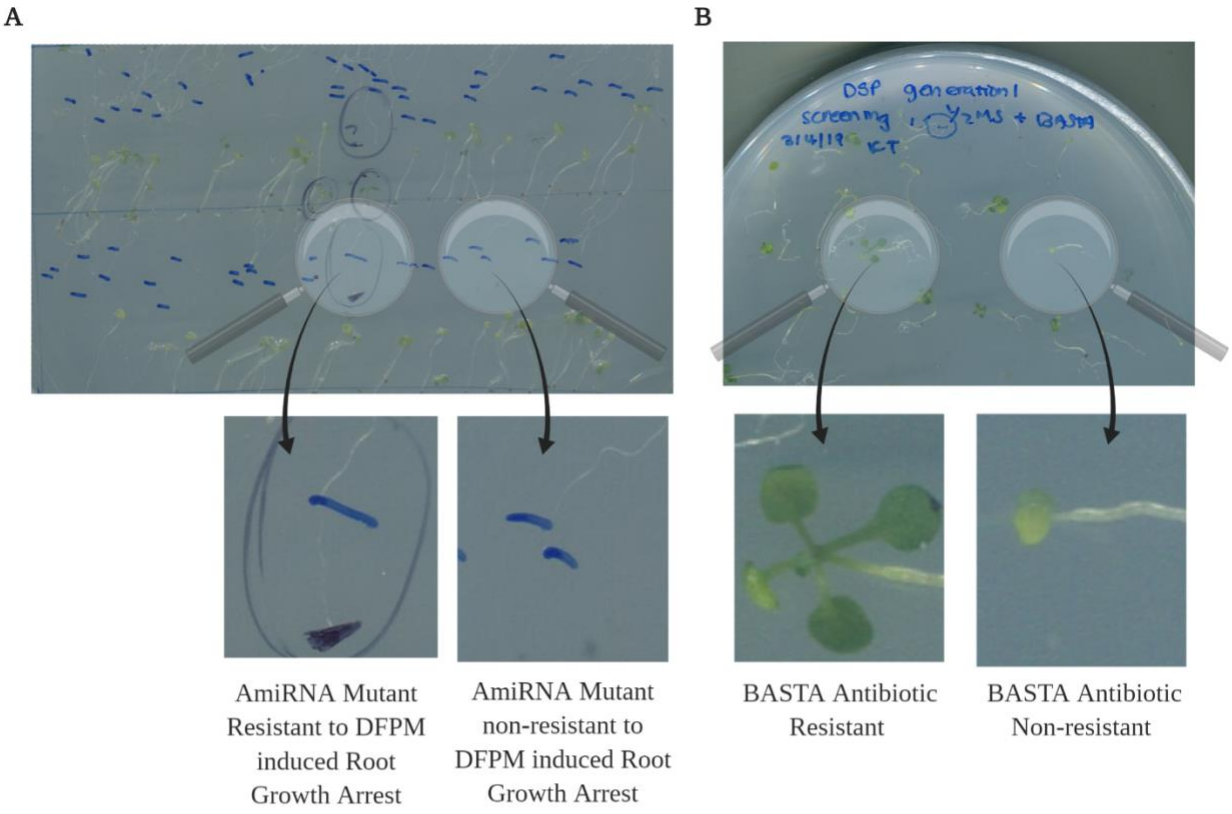
A
B
DSP generation 1
screening
½MS + BASTA
AmiRNA Mutant Resistant to DFPM induced Root Growth Arrest
AmiRNA Mutant non-resistant to DFPM induced Root Growth Arrest
BASTA Antibiotic Resistant
BASTA Antibiotic Non-resistant

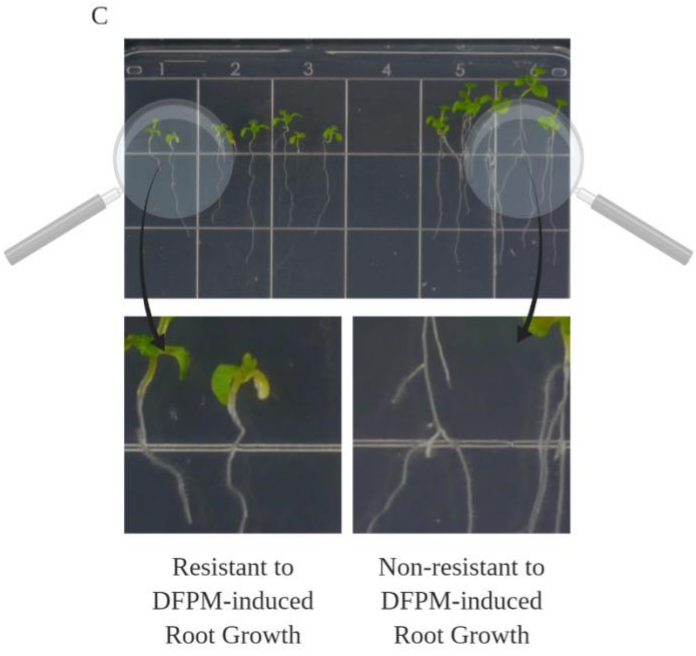
C
Resistant to DFPM-induced Root Growth
Non-resistant to DFPM-induced Root Growth

A AmiRNA Mutant 11 T-3 Control

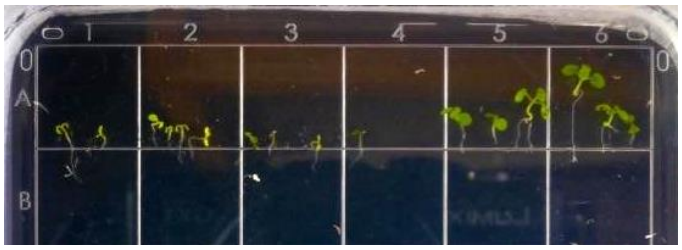

B

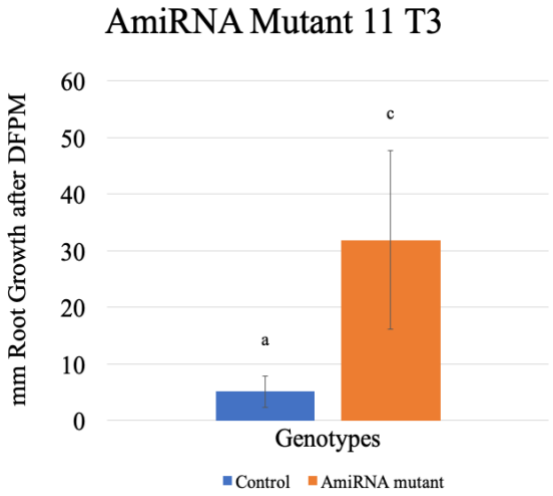

Figure 2.4 Artificial MicroRNA (AmiRNA) Mutant 11 Root Growth Phenotype was demonstrated visually and confirmed via quantification.

A) Seeds from AmiRNA Mutant 11 T3 and Control (amiRNA-HsMyo) were germinated on ½ Murashige and Skoog, 1% sucrose, and 0.8% agar for 8 days then transferred to 10µM DFPM containing ½ Murashige and Skoog, 1% sucrose, and 0.8% agar. Seedlings were aligned such that the bottoms of the roots were on the bottom of Row A in each plate. Images were taken after 4 days of growth on 10µM DFPM media. Seedlings on the left side of the plate are AmiRNA Mutant 11 T3 seedlings, and seedlings on the right are control (amiRNA-HsMyo) seeds acting as control. N = 2, 5-8 seedlings per repeat.
B) Root lengths of AmiRNA Mutant 11 T3 and Control (amiRNA-HsMyo) seedlings were measured via ImageJ software. Error Bars represent standard deviation of data. N = 2, 5-8 seedlings were used for each repeat. The p-value is <0.00001, * indicates P < 0.01, via 1-Way ANOVA.

Table 2.1 Identity of AmiRNA Mutant 11 and target locations was determined to contain the below sequence. This sequence was matched to the PHANTOM library amiRNA sequence targeting At5g063270 and At2g04410, both encoding the RPM1- interacting protein 4 (RIN4) family protein. At5g063270 and At2g04410 derived from the Protein Kinase, Phosphatases, Receptors, and their ligands (PKR) and Unknown Function or cannot be inferred (UNC) amiRNA pools.

amiRNA Sequence	**Targeted Gene Locus**	**Gene Name**	**amiRNA Pool**
TCATTCGCCAAACTTCGGCAT	AT5G63270	RPM1-interacting protein 4 (RIN4) family protein	PKR (Protein Kinase, Phosphatases, Receptors, and their ligands) and UNC (Function is unknown or cannot be inferred)
TCATTCGCCAAACTTCGGCAT	AT2G04410	RPM1-interacting protein 4 (RIN4) family protein	PKR (Protein Kinase, Phosphatases, Receptors, and their ligands) and UNC (Function is unknown or cannot be inferred)

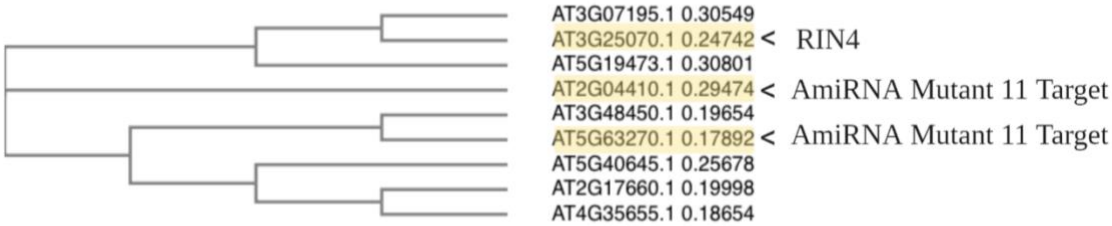

Figure 2.5 Phylogenetic Tree of RIN4 was created via DNA sequence alignment on Simple Phylogeny. The phylogenetic tree of RPM1-interacting protein 4 (RIN4) family protein was constructed to depict the evolutionary relationship between the various family proteins. The arrows mark the published RIN4 sequence and amiRNA mutant targeted RIN4 family protein sequences.

A amiRNA Mutant 12, T3 Control

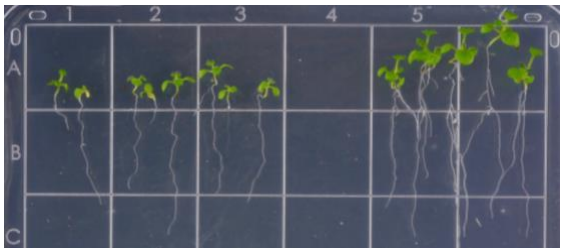

B

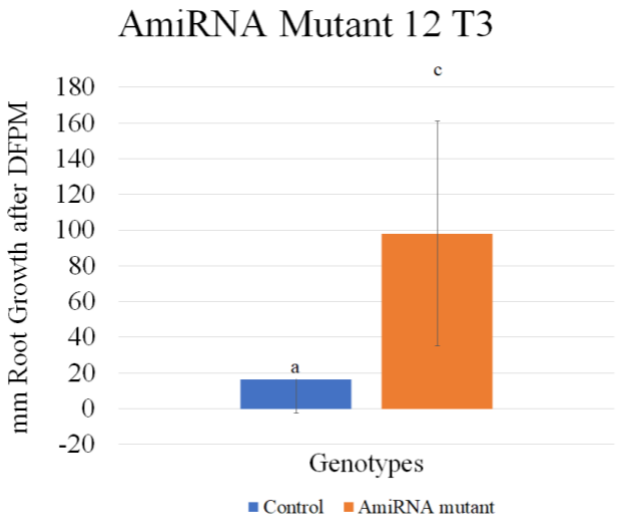

Figure 2.6 Artificial MicroRNA (AmiRNA) Mutant 12 Root Growth Phenotype

(a) Seeds from AmiRNA Mutant 12 T3 and control (amiRNA-HsMyo amiRNA-HsMyo) were germinated on ½ Murashige and Skoog, 1% sucrose, and 0.8% agar for 8 days then transferred to 10µM DFPM containing ½ Murashige and Skoog, 1% sucrose, and 0.8% agar. Seedlings were aligned such that the bottoms of the roots were on the bottom of Row A in each plate. Images were taken after 8 days of growth on 10µM DFPM media. Seedlings on the left side of the plate are AmiRNA Mutant 12 T3 seedlings, and seedlings on the right are HsMyo seeds acting as control. N = 3, 8-10 seedlings per repeat.

(b) Quantification of AmiRNA Mutant 12 T3 Root Growth on DFPM Media Root lengths of AmiRNA Mutant 12 T3 and control (amiRNA-HsMyo) seedlings were measured via ImageJ software. Error Bars represent standard deviation of data. N = 3, 8-10 seedlings were used for each repeat. The p-value is <0.00001, letters represent degree significance, via 1-Way ANOVA.

A AmiRNA Mutant 24 T4-1 Control

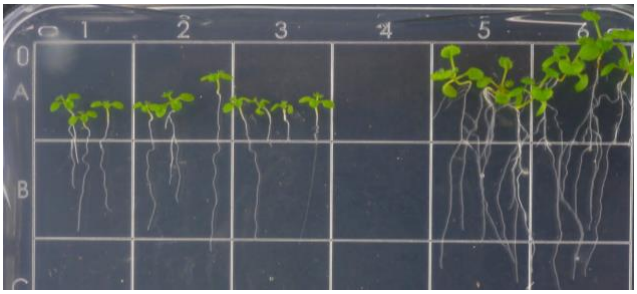

B

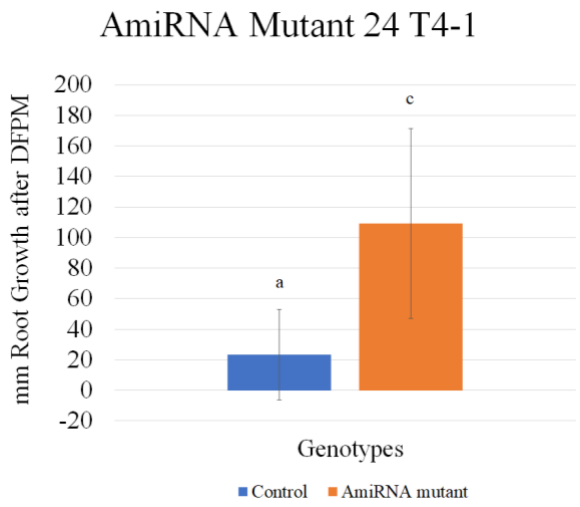

Figure 2.7 AmiRNA Mutant 24 Root Growth Phenotype

A) Seeds from AmiRNA Mutant 24 T4-1 were germinated on ½ Murashige and Skoog, 1% sucrose, and 0.8% agar for 8 days then transferred to 10µM DFPM containing ½ Murashige and Skoog, 1% sucrose, and 0.8% agar. Seedlings were aligned such that the bottoms of the roots were on the bottom of Row A in each plate. Images were taken after 8 days of growth on 10µM DFPM media. Seedlings on the left side of the plate are AmiRNA Mutant 24 T4-1 seedlings, and seedlings on the right are control (amiRNA-HsMyo) acting as control. N = 4, 8-10 seedlings per repeat

B) Root growth of AmiRNA mutant 24 T4-1 and control (amiRNA-HsMyo) seedlings after DFPM exposure were measured via ImageJ software. Error Bars represent standard deviation of data. N = 4, 8-10 seedlings were used for each repeat. The p-value is <0.00001, letters indicates degree significance, via 1-Way ANOVA.

2.4 Discussion

By combining the new forward genetics screening platform of genome targeting artificial microRNA libraries and a [5-(3,4-dichlorophenyl)furan-2-yl]-piperidine-1-ylmethanethione (DFPM) chemical found to induce root growth arrest, we developed a screening method to identify artificial microRNA mutants insensitive to DFPM-induced root growth arrest (Hauser *et al.,* 2013; Hauser *et al.,* 2013; Kim *et al.,* 2012, Kunz *et al.,* 2016).

Protocol Development

Through the successful isolation of mutants 11, 12, and 24 by this novel screening of DFPM induced root growth arrest, we validated the protocol improvements we applied to increase the efficiency of this screening process.

The improvements included preparing the DFPM-containing growth media (½ Murashige and Skoog, 1% sucrose, and 0.8% Agar) ahead of time in an unlit environment, growing the seeds directly on DFPM containing growth media instead of transferring after growth, and blocking photo activation of DFPM activity until proper root growth development. By preparing the plates in an unlit environment and blocking the light-induced bioactivity of DFPM via aluminum foil until appropriate root growth, we have effectively removed the entire transferring step of previous root growth arrest protocols (Kim *et al.,* 2012, Kunz *et al.,* 2016). Experimental findings have demonstrated that seedling growth on DFPM containing media covered in aluminum foil does not interfere with seedling germination or growth; nor does it nullify DPFM bioactivity (Figure 2.3 A) For a large-scale screen where over 500 seeds were grown and tested each week, these were crucial protocol improvements as it reduced the time and energy spent on

transferring individual seedlings, amounts of material utilized, and a significant chance of growth contamination.

One trade off, we believe can still be improved, is the selection of BASTA-resistant mutants. While it is important to select for artificial microRNA constructs in the identified mutants, perhaps that transfer step to BASTA-containing ½ Murashige and Skoog, 0.8% agar is unnecessary. Given that the seeds are grown vertically from the beginning with the roots are exposed, a future avenue for protocol improvement may be exploring different methods of BASTA antibiotic selection directly on the DFPM-containing plates. Perhaps BASTA antibiotic can be directly added to the DFPM-containing ½ Murashige and Skoog, 1% sucrose, and 0.8% plate or directly sprayed onto the roots for selection instead.

Resistant to DFPM-induced root growth arrest amiRNA Mutant 11

The first mutant isolated to demonstrate a repeated resistance to DFPM-induced root growth arrest, amiRNA 11, was identified to target 2 RIN4 related proteins (Table 2.1). This result and its repeated phenotype in two generations indicates that these 2 specific RIN4 family proteins are involved in DFPM-induced root growth arrest. Although these individual RIN4 family proteins have not been characterized in the literature yet, the original RIN4 (At3g25070) (Figure 2.5) was described as a protein that is phosphorylated upon infection by *P. syringae* expressing AvrB or AvrRpm1 and leads to activation of RPM1, a Coiled-coiled (CC) - Nucleotide-Binding (NB) - Leucine Rich Repeat (LRR) Resistant protein, and RPM1-mediated disease resistance (Luderer *et al.,* 2002, Mackey *et al.,* 2002; Mackey *et al.,* 2003). Additionally, the original RIN4 protein has also been published to negatively regulate Resistance to *P.*

syringae 2 (RPS2), another Nucleotide-Binding (NB) - Leucine-Rich Repeat (LRR) protein and RPS2 - mediated disease resistance (Mackey *et al.,* 2003). In summary, our theory is that the RIN4-homologs identified here are critical for DFPM-induced root growth arrest mediated via VICTR, a TIR-NB-LRR protein (Kim et al., 2012, Kunz et al., 2016). Clearly, the relationships between DFPM, VICTR, and our RIN4 homologs need to be studied further. Our RIN4 homologs may act upstream or downstream of VICTR to facilitate DFPM-induced root growth arrest.

Additionally, although the artificial microRNA library we are currently screening encompasses transcription factors and other DNA/RNA binding proteins (TFB), the two microRNA sequences identified were specific to the "protein kinase, phosphatases, receptors, and their ligands" family (PKR) and "function is unknown or can not be inferred" family (UNC) (Table 2.1). Although this may speak to the seed pool purity, it also hints that the PKR and UNC mutant pools may be of interest as well in further dissecting the genetic basis of DFPM-induced root growth arrest.

Experiments currently in progress include the complementation of the artificial microRNA targeting RIN4-related proteins and the testing of RIN4-related protein T-DNA insertion mutant root growth phenotypes. If the complementation assays provide a repeated phenotype of resistant to DFPM-induced root growth arrest, testing the other phylogenetically similar RIN4 family proteins will be of interest in further dissecting this chemical induced cell death signaling pathway.

AmiRNA Mutant 12 and AmiRNA Mutant 24

Artificial microRNA (AmiRNA) mutants 12 and 24 have both exhibited a disruption of DFPM-induced root growth phenotype in at least 2 generations thus far (Figure 2.6, Figure 2.7). The next steps of these mutants are to repeat in the third generation as well as sequence the amiRNA in the mutants to identify the predicted targets of the artificial microRNA constructs within each line. Following, complementation assays should be carried out to ensure this inhibition of DFPM-induced root growth arrest is indeed caused by these gene knockdowns. Then, depending on the roles of the identified gene families, further characterization assays would be recommended.

In summation, the screening protocol developed is efficient in isolating mutants with a robust resistant-to-DFPM phenotype. Small changes such as incorporating BASTA antibiotic into growing methods can be made to lean the screening process in interest of time, labor, and materials utilized. It is suggested to follow up with these changes in further development of this protocol while continuing to screen the transcription factors and Protein Kinases library of artificial microRNA mutants. The mutants identified through this screen require proper complementation of re-transformation of the artificial microRNA construct into wild-type seeds in order to confirm the silenced genes' participation in DFPM-induced root growth arrest. Following confirmation via complementation, it will be of interest to test knock out mutants of the genes, higher order mutants based on genetic homology, and gene expression assays to further characterize how the identified genes may fit in as a puzzle piece to the cell death signaling pathway.

References

Axtell, M. J., & Staskawicz, B. J. (2003). Initiation of RPS2-specified disease resistance in Arabidopsis is coupled to the AvrRpt2-directed elimination of RIN4. *Cell*, *112*(3), 369–377. https://doi.org/10.1016/S0092-8674(03)00036-9

Bakker, E. G., Toomajian, C., Kreitman, M., & Bergelson, J. (2006). A genome-wide survey of R gene polymorphisms in Arabidopsis. *Plant Cell*, *18*(8), 1803–1818. https://doi.org/10.1105/tpc.106.042614

Belkhadir, Y., Nimchuk, Z., Hubert, D. A., Mackey, D., & Dangl, J. L. (2004). Arabidopsis RIN4 negatively regulates disease resistance mediated by RPS2 and RPM1 downstream or independent of the NDR1 signal modulator and is not required for the virulence functions of bacterial type III effectors AvrRpt2 or AvrRpm1. *Plant Cell*, *16*(10), 2822–2835. https://doi.org/10.1105/tpc.104.024117

Cohn, J., Sessa, G., & Martin, G. B. (2001). Innate immunity in plants. *Current Opinion in Immunology*. https://doi.org/10.1016/S0952-7915(00)00182-5

Coll, N. S., Epple, P., & Dangl, J. L. (2011, August). Programmed cell death in the plant immune system. *Cell Death and Differentiation*. https://doi.org/10.1038/cdd.2011.37

Dangl, J. L., & Jones, J. D. G. (2001, June 14). Plant pathogens and integrated defence responses to infection. *Nature*. https://doi.org/10.1038/35081161

Eliceiri, K., Schneider, C. A., Rasband, W. S., & Eliceiri, K. W. (2012). NIH Image to ImageJ : 25 years of image analysis HISTORICAL commentary NIH Image to ImageJ : 25 years of image analysis. *Nature Methods*, *9*(7), 671–675. https://doi.org/10.1038/nmeth.2089

Gassmann, W., & Bhattacharjee, S. (2012). Effector-Triggered Immunity Signaling: From Gene-for-Gene Pathways to Protein-Protein Interaction Networks. *Molecular Plant-Microbe Interactions MPMI*, *25*(7). https://doi.org/10.1094/MPMI

Greenberg, J. T. (1997). PROGRAMMED CELL DEATH IN PLANT-PATHOGEN INTERACTIONS. *Annual Review of Plant Physiology and Plant Molecular Biology*, *48*(1), 525–545. https://doi.org/10.1146/annurev.arplant.48.1.525

Greenberg, J. T. (2002). Programmed Cell Death in Plant-Pathogen Interactions. *Annual Review of Plant Physiology and Plant Molecular Biology*. https://doi.org/10.1146/annurev.arplant.48.1.525

Hammond-Kosack, K. E., & Jones, J. D. G. (1996, October). Resistance gene-dependent plant defense responses. *Plant Cell*. https://doi.org/10.1105/tpc.8.10.1773

Hauser, F., Ceciliato, P., Lin, Y. C., Guo, D., Gregerson, J., Abbasi, N., Youhanna, D., Park, J., Dubeaux, G., Shani, E., Poomchongkho, N., Schroeder, J. I. (2019). A seed resource for screening functionally redundant genes and isolation of new mutants impaired in CO2 and ABA responses. *Journal of Experimental Botany*, *70*(2), 641–651. https://doi.org/10.1093/jxb/ery363

Hauser, F., Chen, W., Deinlein, U., Chang, K., Ossowski, S., Fitz, G., Hannon, B., Schroeder, J. I. (2013). A genomic-scale artificial MicroRNA library as a tool to investigate the functionally redundant gene space in arabidopsis. *Plant Cell*, *25*(8), 2848–2863. https://doi.org/10.1105/tpc.113.112805

Jones, J. D. G., & Dangl, J. L. (2006, November 16). The plant immune system. *Nature*. https://doi.org/10.1038/nature05286

Kabbage, M., Kessens, R., Bartholomay, L. C., & Williams, B. (2017). The Life and Death of a Plant Cell. *Annual Review of Plant Biology*, *68*(1), 375–404. https://doi.org/10.1146/annurev-arplant-043015-111655

Kim, T.-H., Kunz, H.-H., Bhattacharjee, S., Hauser, F., Park, J., Engineer, C., Liu, A., Ha, T., Parker, J. E., Gassmann, W., Schroeder, J. I. (2012). Natural Variation in Small Molecule-Induced TIR-NB-LRR Signaling Induces Root Growth Arrest via EDS1- and PAD4-Complexed R Protein VICTR in Arabidopsis. *The Plant Cell*, *24*(12), 5177–5192. https://doi.org/10.1105/tpc.112.107235

Kim, T.-H., Hauser, F., Ha, T., Xue, S., Böhmer, M., Nishimura, N., Munemasa, S., Hubbard, K., Peine, N., Lee, B.H., Lee, S., Robert N., Parker, J.E., Schroeder, J. I. (2011). Chemical genetics reveals negative regulation of abscisic acid signaling by a plant immune response pathway. *Current Biology : CB*, *21*(11), 990–997. https://doi.org/10.1016/j.cub.2011.04.045

Kunz, H. H., Park, J., Mevers, E., García, A. V., Highhouse, S., Gerwick, W. H., Parker, J.E., Schroeder, J. I. (2016). Small molecule DFPM derivative-activated plant resistance protein signaling in roots is unaffected by EDS1 subcellular targeting signal and chemical genetic isolation of VICTR R-protein mutants. *PLoS ONE*, *11*(5), 1–20. https://doi.org/10.1371/journal.pone.0155937

Luderer, R., & Joosten, M. H. A. J. (2001). Avirulence proteins of plant pathogens: Determinants of victory and defeat. *Molecular Plant Pathology*. https://doi.org/10.1046/j.1464-6722.2001.00086.x

Mackey, D., Belkhadir, Y., Alonso, J. M., Ecker, J. R., & Dangl, J. L. (2003). Arabidopsis RIN4 is a target of the type III virulence effector AvrRpt2 and modulates RPS2-mediated resistance. *Cell*, *112*(3), 379–389. https://doi.org/10.1016/s0092-8674(03)00040-0

Mackey, D., Holt, B. F., Wiig, A., & Dangl, J. L. (2002). RIN4 interacts with Pseudomonas syringae type III effector molecules and is required for RPM1-mediated resistance in Arabidopsis. *Cell*, *108*(6), 743–754. https://doi.org/10.1016/S0092-8674(02)00661-X

Maekawa, T., Kufer, T. A., & Schulze-Lefert, P. (2011, September). NLR functions in plant and animal immune systems: So far and yet so close. *Nature Immunology*. https://doi.org/10.1038/ni.2083

Martin, G. B., Bogdanove, A. J., & Sessa, G. (2003). U NDERSTANDING THE F UNCTIONS OF P LANT D ISEASE R ESISTANCE P ROTEINS . *Annual Review of Plant Biology*, *54*(1), 23–61. https://doi.org/10.1146/annurev.arplant.54.031902.135035

McHale, L., Tan, X., Koehl, P., & Michelmore, R. W. (2006, April 26). Plant NBS-LRR proteins: Adaptable guards. *Genome Biology*. https://doi.org/10.1186/gb-2006-7-4-212

Meyers, B. C., Kozik, A., Griego, A., Kuang, H., & Michelmore, R. W. (2003). Genome-wide analysis of NBS-LRR-encoding genes in Arabidopsis. *Plant Cell*, *15*(4), 809–834. https://doi.org/10.1105/tpc.009308

Opin, C., Biol, P., Ellis, J., Dodds, P., & Pryor, T. (2017). Ellis , J ., Dodds , P . & Pryor , T . Structure , function and evolution of plant disease resistance genes . Structure , function and evolution of plant disease resistance genes, (September 2000), 278–284. https://doi.org/10.1016/S1369-5266(00)00080-7

Park, J., Kim, T. H., Takahashi, Y., Schwab, R., Dressano, K., Stephan, A.B., Ceciliato P.H.O., Ramirez, E., Garin, V., Huffaker, A., Schroeder, J. I. (2019). Chemical genetic identification of a lectin receptor kinase that transduces immune responses and interferes with abscisic acid signaling. *Plant Journal*, 1–19. https://doi.org/10.1111/tpj.14232

Pieterse, C. M. J., Leon-Reyes, A., Van Der Ent, S., & Van Wees, S. C. M. (2009). Networking by small-molecule hormones in plant immunity. *Nature Chemical Biology*. Nature Publishing Group. https://doi.org/10.1038/nchembio.164

Richly, E., Kurth, J., & Leister, D. (2002). Mode of amplification and reorganization of resistance genes during recent Arabidopsis thaliana evolution. *Molecular Biology and Evolution*, *19*(1), 76–84. https://doi.org/10.1093/oxfordjournals.molbev.a003984

Schindelin, J., Rueden, C. T., Hiner, M. C., & Eliceiri, K. W. (2015, July 1). The ImageJ ecosystem: An open platform for biomedical image analysis. *Molecular Reproduction and Development*. John Wiley and Sons Inc. https://doi.org/10.1002/mrd.22489

Takken, F. L. W., & Tameling, W. I. L. (2009, May 8). To nibble at plant resistance proteins. *Science*. https://doi.org/10.1126/science.1171666

Takken, F. L., Albrecht, M., & Tameling, W. IL. (2006, August). Resistance proteins: molecular switches of plant defence. *Current Opinion in Plant Biology*. https://doi.org/10.1016/j.pbi.2006.05.009

Wagner, A. (2005, February). Distributed robustness versus redundancy as causes of mutational robustness. *BioEssays*. https://doi.org/10.1002/bies.20170

Warren, R. F., Henk, A., Mowery, P., Holub, E., & Innes, R. W. (1998). A mutation within the leucine-rich repeat domain of the arabidopsis disease resistance gene RPS5 partially suppresses multiple bacterial and downy mildew resistance genes. *Plant Cell*, *10*(9), 1439–1452. https://doi.org/10.1105/tpc.10.9.1439